



Munich Personal RePEc Archive

# **Poverty, pollution, and mortality: The 1918 influenza pandemic in a developing German economy**

Franke, Richard

University of Bayreuth

2021

Online at <https://mpra.ub.uni-muenchen.de/107570/>  
MPRA Paper No. 107570, posted 22 May 2021 00:17 UTC

# Poverty, Pollution, and Mortality: The 1918 Influenza Pandemic in a Developing German Economy

Richard Franke\*  
University of Bayreuth

May 18, 2021

## Abstract

The paper provides a detailed analysis of excess mortality during the “Spanish Flu” in a developing German economy and the effect of poverty and air pollution on pandemic mortality. The empirical analysis is based on a difference-in-differences approach using annual all-cause mortality statistics at the parish level in the Kingdom of Württemberg. The paper complements the existing literature on urban pandemic severity with comprehensive evidence from mostly rural parishes. The results show that middle and high-income parishes had a significantly lower increase in mortality rates than low-income parishes. Moreover, the mortality rate during the 1918 influenza pandemic was significantly higher in highly polluted parishes compared to least polluted parishes.

**Keywords:** Pandemics, Spanish Flu, Income, Air Pollution, Mortality

**JEL Classification:** I14, I15, N34, Q53

**Acknowledgements:** I thank seminar and conference participants at the University of Bayreuth, the Economic History Society Annual Conference, the Congress on Economic and Social History, as well as Martin Baur, Sebastian Braun, and David Stadelmann for their valuable comments. Elisa Poletto and Sarah Stricker provided excellent research assistance. All remaining errors are my own.

---

\*University of Bayreuth, Faculty of Law, Business and Economics, 95440 Bayreuth, Germany. Email: richard.franke@uni-bayreuth.de. Tel.: +49 (0) 921 55 6224.

# 1 Introduction

The 1918 “Spanish Flu” was the most deadly influenza pandemic in modern history, likely causing 50–100 million deaths (Johnson and Mueller, 2002). Besides the large range in the global mortality estimates, the local mortality rate estimates show enormous variation across and within countries.<sup>1</sup> To date, the factors influencing the varying regional severity of the pandemic have not been fully explored. This paper studies the local determinants of pandemic mortality in southwest Germany, using exceptionally detailed vital statistics for 1,763 parishes in the German Kingdom of Württemberg. The analysis focuses on the effect of poverty and air pollution on mortality. Both factors have received much attention also in current debates on regional differences in pandemic mortality (Beach et al., 2020; Wu et al., 2020).

The paper makes three contributions to the literature on regional differences in pandemic severity during the 1918 influenza pandemic. First, I study the determinants of pandemic severity at an unusually disaggregated level: the median land area of parishes in the sample is just 8.6 square kilometers, and the median population is 649. The analysis thus complements the existing literature on urban pandemic severity with comprehensive evidence from mostly rural parishes. The focus on rural parishes is essential because previous results indicate considerable differences in pandemic severity by the degree of urbanization (e.g. Clay et al., 2019). Second, I provide the first analysis on the effect of income on regional pandemic severity for Germany and one of the first for continental Europe. This point is important as existing evidence points to significant differences in pandemic severity between Europe and the US (Bootsma and Ferguson, 2007). Moreover, in contrast to the analysis for the US (Bootsma and Ferguson, 2007; Clay et al., 2018, 2019; Grantz et al., 2016), recent studies focusing on Europe provide mixed evidence on the effect of income on influenza mortality (Karlsson et al., 2014; Dahl et al., 2020; Carillo and Jappelli, 2020). Third, I assess the link between air pollution and regional pandemic mortality, motivated by considerable evidence that air pollutants can increase susceptibility to influenza infection (e.g., Jaspers et al., 2005).

Furthermore, the paper provides a detailed description of mortality statistics in Württemberg. The official statistics are disaggregated by cause of death, age, and sex. For instance, the reported influenza mortality did increase by about 3,000 percent in 1918 compared to previous years and showed a distinctive W-shape in the age-specific mortality pattern. To the best of my knowledge, data with a comparable level of detail have not been discussed for any major German state before.<sup>2</sup> The paper also relates the excess mortality rate estimates for Württemberg to

---

<sup>1</sup>For example, Johnson and Mueller (2002) estimate country specific mortality rates between 1.2 and 445.0 per 1,000 persons, for Argentina and Cameroon, respectively, and Bootsma and Ferguson (2007) estimate 4–12 excess deaths per 1,000 persons in a sample of 47 US cities.

<sup>2</sup>Previous studies of the 1918 influenza pandemic in Germany often focus on case studies for smaller areas or the medical debates of the time (Michels, 2010).

newly estimated excess mortality rates of Germany and its states. Based on these estimates, the paper shows an association of income and air pollution at the national level. Moreover, the paper briefly describes the socio-economic conditions in Württemberg at the beginning of the 20th century and the adverse effects of World War I (WWI) on food supply and pre-pandemic health. The suffering caused by WWI may also explain why the 1918 influenza pandemic did not leave a lasting impression on the collective memory of the German population.

For the empirical analysis, I use annual data on vital statistics (all-age and infant mortality, births) for the universe of parishes in Württemberg in 1914–1925. I combine these data with rich socio-economic data from various population and occupation censuses. For each parish, I observe the amount of total taxable income in 1907 and calculate the average income per capita. In addition, I link the data with available information on the location of coal-fired power plants, a major source of air pollution in the early 20th century (Clay et al., 2018).<sup>3</sup> Before WWI, about two-thirds of the installed power plant capacity in Württemberg and neighboring Hohenzollern was based on coal (Ott et al., 1981). The pollution was spatially dispersed from the power plants and affected the pollution levels of parishes in a wider radius. I exploit this fact to calculate the exposure of each parish to pollution from coal-fired power plants.

The empirical analysis is based on a difference-in-differences approach to estimate the effect of poverty and air pollution on pandemic mortality. The approach compares mortality rate changes in poor (least polluted) parishes to mortality rate changes in rich (highly polluted) parishes. The average all-cause mortality rate across parishes in Württemberg was 15.8 deaths per 1,000 persons during the pandemic year 1918, corresponding to a mortality rate increase of 2.9 deaths or 23 percent relative to the baseline in 1917.

The results show that middle and high-income parishes (classified by taxable income per capita) recorded a significantly lower increase in mortality rates than low-income parishes. The respective increase in the mortality rate in medium and high-income parishes was lower by 1.4 and 1.0 deaths per 1,000 population. Moreover, the mortality rate increase from 1917 to 1918 was significantly higher in highly polluted parishes compared to least polluted parishes. The estimates indicate an additional increase in the mortality rate by 1.0 death per 1,000 population. In other words, the spike in 1918 mortality was particularly large in poor and highly polluted parishes.

Two recent articles summarize the extensive literature on the effects of the 1918–1919 influenza pandemic. Beach et al. (2020) focus on literature about economic and health outcomes, and Taubenberger et al. (2019) focus on the medical and biological insights on the 1918 in-

---

<sup>3</sup>There are no data on the actual air pollution levels in Württemberg available for the time period. However, the level of pollution in the late 19th and early 20th century in industrialized countries is considered to be much higher than today and mainly caused by the usage of coal (Bailey et al., 2018; Beach and Hanlon, 2017).

fluenza pandemic. The review articles demonstrate that although an extensive body of work has emerged over the last century, numerous questions remain unanswered to date, not least on the origin of the virus and how many deaths it caused. Widely cited estimates on the global mortality burden range between 50 and 100 million deaths (Johnson and Mueller, 2002). This large range in estimates is partially driven by sparse data for developing countries in Africa and Asia, especially China.<sup>4</sup> However, even for industrialized countries that generally have detailed statistics in the early 20th century, the estimates vary strongly. For example, the excess all-cause mortality rate is estimated between 3.9 and 6.5 deaths per 1,000 persons for the USA, between 2 and 4.1 for Denmark, and between 3.8 and 7.8 for Germany (Beach et al., 2020). According to new estimates in this paper, the excess mortality rate for Germany was between 5.4 and 5.9 and Württemberg might have experienced up to 4.1 excess deaths per 1,000 persons.

The empirical analysis focuses on the impact of poverty and air pollution on mortality. Both factors have received much attention also in debates on regional differences in mortality during the COVID-19 pandemic. Several studies have analyzed the effect of socio-economic differences on mortality during the 1918 influenza pandemic. However, some of these studies do not study income, but other potentially correlated measures like apartment size (Mamelund, 2006, 2018), social status based on occupation (Bengtsson et al., 2018), and housing conditions (Sydenstricker, 1931; Chowell et al., 2007), or illiteracy rates, home ownership, and unemployment (Clay et al., 2019; Grantz et al., 2016). These papers provide evidence for a socio-economic gradient in mortality rates during the 1918 influenza pandemic. However, the measures used in these studies focus on a specific channel of the income effect. This limitation is not trivial because income differences can affect pandemic mortality through multiple channels, and the studies mentioned above potentially neglect parts of the effect.<sup>5</sup>

Focusing on cross-country differences in income, Murray et al. (2006) and Barro et al. (2020) find a significant negative income effect on pandemic mortality in a sample of 27 and 42 countries, respectively.<sup>6</sup> Other studies, however, do not find a significant correlation between income levels and pandemic mortality 1918, e.g., Brainerd and Siegler (2003) for US states, Karlsson et al. (2014) for Swedish counties, and Carillo and Jappelli (2020) for Italian regions. Using Danish municipality level data, Dahl et al. (2020) show that the epidemic intensity in 1918 does not depend on differences in income levels four or more years before the pandemic, but differences

---

<sup>4</sup>The actual range of mortality estimates is even larger, e.g., Patterson and Pyle (1991) estimate a global mortality burden of 25–40 million deaths.

<sup>5</sup>Differences in income can affect multiple factors that influence (pandemic) mortality, like the nutritional situation (Blum, 2013), access to sanitary infrastructure (Gallardo-Albarrán, 2020), or access to healthcare (Bauernschuster et al., 2020). For instance, it is not clear to what extent these factors are captured by social status differences of individuals. See Deaton (2003) and Weil (2014) for a detailed discussion on the association between income differences and health.

<sup>6</sup>Basco et al. (2021) use Spanish occupation level data and associated income to show a negative association between income and pandemic mortality rates. Furthermore, Clay et al. (2018) control for the manufacturing payroll per worker in 1900, but the results for this estimator are not reported.

in income levels 1917 and income growth from 1916 to 1917.

The literature provides strong evidence on the effect of socio-economic factors, but the effect of income level differences on pandemic mortality is less well understood. In this paper, I show that the income level in 1907 has a statistically and epidemiologically significant effect on the relative change in all-cause mortality rates between 1917 and 1918. I provide evidence that parishes with lower income levels in 1907 experienced a significantly stronger increase in mortality rates from 1917 to 1918. The level of analysis is of particular interest because there is empirical evidence that the influenza pandemic had different impacts in smaller and more rural parishes (Acuna-Soto et al., 2011; Chowell et al., 2007).

The effect of pollution on mortality during the 1918 influenza pandemic has received less attention.<sup>7</sup> Only recently, an article by Clay et al. (2018) shows the effect of installed coal-fired electricity generating capacity on mortality in a sample of 180 US cities. The authors find the mortality rate to increase by an additional 9.6 percent in high-capacity cities and by 5.4 percent in medium capacity cities, relative to changes in low-capacity cities. Furthermore, Clay et al. (2018) find a significant effect of pollution on infant mortality. In an extended data set of 438 US cities with at least 10,000 inhabitants, Clay et al. (2019) test the effect of multiple factors on excess mortality in 1918, including coal-fired capacity. Their results confirm the significant effect of pollution on pandemic mortality, but only for high-capacity cities.

The empirical strategy of the paper follows mainly Clay et al. (2018). The main difference, however, is the unit of analysis. Clay et al. (2018) use a sample of US cities with at least 20,000 inhabitants, while the median parish in Württemberg has a population of 649 inhabitants. The paper also contributes to a broader literature that analyzes the effect of pollution on (infant) mortality, e.g., Chay and Greenstone (2003) and Currie and Neidell (2005), who study the effect of pollution on infant mortality in the modern-day US, and Beach and Hanlon (2017), who analyzes the effect of pollution on mortality during the Industrialization in England and Wales.

The paper is structured as follows. Section 2 describes the socio-economic conditions in Württemberg and the influence of World War I on living conditions, as well as the statistics on influenza and excess mortality during the 1918–1919 influenza pandemic in Württemberg. Furthermore, Section 2 compares the excess mortality estimates with new estimates for Germany and provides first evidence on the effect of income and air pollution on regional pandemic severity at the national level. Section 3 describes the data used in the empirical analysis on the effect of income and pollution on pandemic mortality rates. Section 4 discusses the identification strategy and Section 5 reports the main results together with several robustness checks before Section 6 concludes.

---

<sup>7</sup>The detrimental health effects of pollution on influenza in general, however, have been studied more extensively, see for example Jaspers et al. (2005), Wong et al. (2009), and Wu et al. (2020).

## 2 World War I and the “Spanish Flu” in Württemberg

On October 19, 1918, the military physician assistant (*Feldhilfsarzt*) Erich Steinthal from Stuttgart published an article about the new “Spanish Disease”. Steinthal (1918) closes his article with a warning that although the press in Württemberg has taken the influenza outbreak lightly, the pandemic’s overall consequences cannot be foreseen. The article, published at the peak of the 1918 influenza pandemic in Stuttgart (the capital of the Kingdom of Württemberg), illustrates the perception of the pandemic as a minor problem in local media. The low level of media and public interest in the pandemic was due to the (self-)censorship of the press and the hardships of everyday survival imposed by the First World War (Witte, 2003). In the following, I describe the socio-economic conditions before and during the Great War and the course of the 1918–1919 influenza pandemic in Württemberg.

### 2.1 The state of Württemberg’s economic development

The Kingdom of Württemberg was one of the four Kingdoms of the German Empire and the third largest after Prussia and Bavaria (see Figure A-1 in the Appendix). According to the 1910 census, Württemberg had a population of about 2.4 million. Württemberg was a latecomer in the Industrial Revolution and its industrialization process still lagged behind other German states at the beginning of the 20th century (Marquardt, 1985; Flik, 2001). The share of agricultural employment in Württemberg was 41.3 percent in 1907, while on average in the German Empire, it was 32.7 percent (Losch, 1912). In addition, Frank (1993) estimates the GDP per capita in 1913 to be 672.26 *Mark* in Württemberg, 745.52 *Mark* in Prussia, and 710.28 *Mark* in neighboring Baden. The aggregate figures, however, mask considerable heterogeneity within Württemberg. The Kingdom comprised four districts (*Kreise*), and the most developed district, the *Neckarkreis*, had a GDP per capita of 766.8 *Mark* and an agricultural employment share of 33.1 percent in 1907.

Economic historians have identified multiple factors that contributed to the economic backwardness of the Kingdom. One factor is the institutional setting of Württemberg, especially the relatively late abolition of guilds in 1862 (Acemoglu et al., 2011; Ogilvie, 2004, 2019) and the division of property among all heirs (*Realteilung*), which caused fragmentation of property and reduced the mobility of labor (Flik, 2001). Before the construction of railways, Württemberg’s economy also faced high transport costs due to the lack of navigable waterways and the hilly topography (Braun and Franke, 2019). In addition, the Kingdom lacked raw materials, such as coal or ore, that have been key drivers in early industrialization (Fernihough and O'Rourke, 2020). In 1913, for example, about 1,000 kilograms of coal were consumed per capita in Württemberg, compared with an average of 3,870 kilograms per capita in the whole German Empire

(Statistisches Landesamt, 1923; Statistisches Reichsamt, 1925).

Despite the lack of coal deposits, the public electricity supply in Württemberg before WWI was considered very advanced compared to other German states. An official report states that out of the 1,907 parishes and localities, 1,705 had a sufficient supply of electricity in March 1915 (Ott, 1971). The parishes were served by 273 power plants in 1916, and about two-thirds of the installed power plant capacity in Württemberg and neighboring Hohenzollern was based on coal (Ott, 1971; Ott et al., 1981). Already in 1903, more than 15 percent of the installed steam capacity in Württemberg was used in electric power plants.<sup>8</sup> With additional power plants completed until 1914, the share of steam engines used for electric power generation increased even further (Ott, 1971). Moreover, WWI did not affect energy production strongly. Statistics show that the usage of coal in Württemberg was 1,000 kilograms per capita in 1913 but 1,037 kilograms of coal per capita in 1918 (Statistisches Landesamt, 1923).<sup>9</sup>

## 2.2 The First World War and food shortages

When the German Empire declared war on Russia on August 1, 1914, there was hardly any publicly noticeable criticism (Herwig, 2014). This changed soon, however, with missing success in military campaigns and an ever prolonging war. In the German Empire, about 2 million soldiers lost their lives, and more than 4 million were wounded during the First World War (Statistisches Reichsamt, 1925). In Württemberg, more than 72,000 soldiers died during the war, with over 5,000 deaths due to diseases (Statistisches Landesamt, 1922).<sup>10</sup> Thus, the military losses account for about 3 percent of Württemberg's pre-war population and 14 percent of males of military age (17–45 years old).

The suffering due to WWI, however, was not limited to the soldiers and their families but reached the whole population. Cox (2015) uses data of school-age children in Germany during WWI, and Blum (2011, 2013) uses anthropomorphic data from German World War II soldiers to show severe malnutrition in Germany during WWI. There are multiple reasons for the crisis of food supply. First, the demand of the military for soldiers and draft animals lowered agricultural productivity. For instance, the number of horses in Württemberg decreased by 32 percent between December 1913 and December 1914 (Statistisches Landesamt, 1923). Second, the Allied blockade hindered much-needed agricultural imports to Germany (Howard, 1993). Before WWI,

---

<sup>8</sup>In 1903, there was about 11 MW of installed coal-fired power plant capacity, or about 15,000 horsepower in Württemberg (Ott et al., 1981). Based on a workplace census in 1902, the installed total steam capacity was 102,391 horsepower, including the installed capacity of electric power plants (Königliches Statistisches Landesamt, 1905). The share of steam engines used in electric power generation was likely above 15 percent, because the 11 MW of installed capacity in coal-fired power plants (*Dampfkraftwerke*) excludes steam power in electric power plants that used multiple sources for energy generation in combination with steam (*gemischter Antrieb*).

<sup>9</sup>See Section A.2 in the Appendix for a more detailed discussion of coal consumption and electricity production during WWI.

<sup>10</sup>Later official statistics report an even higher death toll of 74,026 (Statistisches Landesamt, 1928).

Germany was the largest importer of agricultural products in the world (Blum, 2013). However, Germany not only imported agricultural products for immediate consumption but also fertilizers. Thus, the blockade had an additional negative impact on agricultural productivity. Third, the increasing demand for military products diverted further labor, including women, from agriculture to manufacturing. Finally, crop failures increased food shortages. Most prominently, the potato crop failure of 1916, in combination with the harsh winter of 1916–1917, caused many civilian deaths due to starvation and related diseases. Grebler and Winkler (1940) estimate that 424,000 German civilians died due to starvation during WWI.<sup>11</sup>

German authorities made several attempts to cope with the food crisis. In 1916 the *Kriegsernährungsamt* was founded. This new state agency should coordinate the efforts of a secure food supply. Measures included the introduction of price ceilings and food rationing. The measures by the government, however, could not increase the food supply and might have even caused the opposite. Blum (2013) describes that the prices for meat relative to other staple products were distorted, such that farmers started to feed staple products to livestock. At the same time, a black market arose, allowing more wealthy people to stock food and thus increase food shortages, especially for poor households (Howard, 1993).

The increasingly hopeless military situation and food shortages facilitated the Kiel mutiny on November 3, 1918. It was the starting point of the German Revolution that ended the German Monarchy within a few days and intensified the calls for peace. On November 11, the Armistice of Compiègne ended the First World War's battles. However, the conditions during the revolutionary period did not improve immediately, partly because the blockade ended only in July 1919.

### **2.3 The mortality burden of the influenza pandemic**

In this situation of war and food shortages, the 1918–1919 influenza pandemic reached Württemberg. Figure 1 illustrates the monthly number of all-cause deaths for the Kingdom of Württemberg and the capital Stuttgart (Statistisches Landesamt, 1922). The virus that caused the influenza pandemic might have already spread before 1918, but the excess mortality only exceeded detection thresholds worldwide in 3 waves in 1918 and 1919 (Johnson, 2001; Taubenberger et al., 2019). The first wave in northern spring and summer 1918, the second wave in autumn 1918, and the third wave in spring 1919. In line with this pattern, the first wave of the influenza pandemic in Württemberg peaked in July 1918.<sup>12</sup> The overall number of monthly deaths, excluding military personnel and stillbirths, increased from 2,688 in June 1918 to 3,133 in July

---

<sup>11</sup>Other contemporaneous sources estimate an even higher death toll of over 700,000 deaths due to starvation (Cox, 2015). However, this figure might have been exaggerated for political reasons.

<sup>12</sup>Bogusat (1923) notes that the first influenza infections in Württemberg were recorded already in March 1918. These are the earliest records of influenza infections in the German Empire.

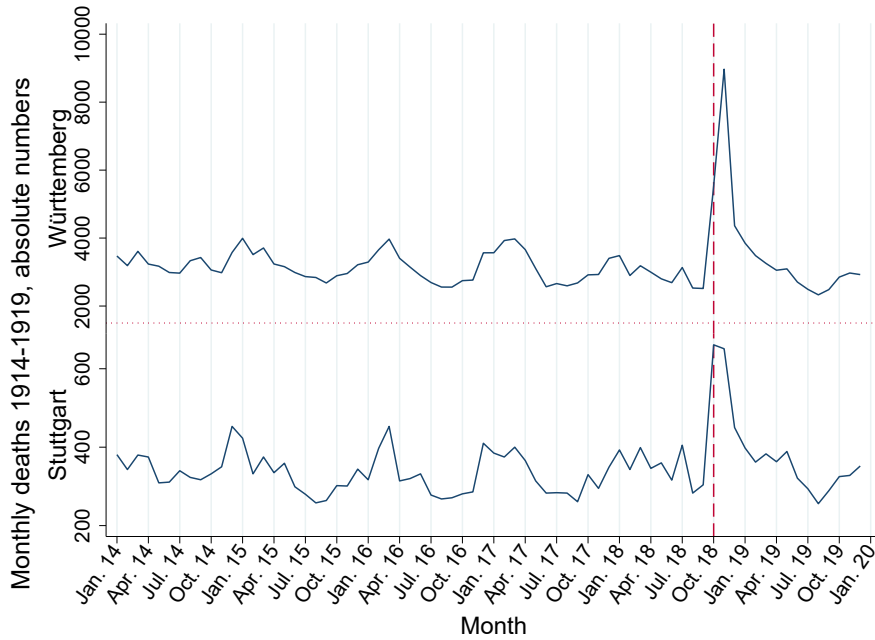


**Figure 1:** Absolute number of monthly deceased 1914–1919

*Notes:* The graph depicts monthly total deceased in the Kingdom of Württemberg (upper graph) and the capital Stuttgart (bottom graph) for the years 1914–1919. The number of deceased does not include military personnel and stillbirths. *Source:* Statistisches Landesamt (1922). Author’s design.

1918. The average number of monthly deceased in July for the years 1914 to 1917 is 2,798. Thus, Württemberg has seen an increase in monthly deaths of 17 percent (relative to June 1918) or 12 percent (relative to July 1914–1917). The spike in July 1918 is even more pronounced in Stuttgart, where the number of monthly death increased by 28 or 37 percent, respectively. The big difference in both measures for Stuttgart might indicate that the influenza pandemic hit the city already in June 1918.

The second, more deadly wave of the influenza pandemic spread in Württemberg in October 1918, marked by the vertical dashed line in Figure 1. The second wave peaked in November 1918, when the total number of deaths increased to 8,969, an increase of 208 percent relative to the average November 1914–1917. The peak in Stuttgart, however, was already reached in October 1918. Thus, the peak of the second wave of the pandemic was earlier in the capital. This observation fits the well-documented pattern of the spread of the 1918 influenza pandemic, i.e., a spread from more central urban hubs to the rural hinterlands (Clay et al., 2019). Finally, Figure 1 reveals the effects of a third wave that spread in Württemberg in April and May 1919, with a peak in overall mortality in May. The magnitude of the third wave is comparable to the first wave, but it was the second wave that was the most severe.

A similar picture is drawn by Figure 2, where the solid line depicts the number of deceased infants under age one per 1,000 births in a given month within Württemberg and the dashed line the total number of births per month. Although the infant mortality rate shows higher volatility

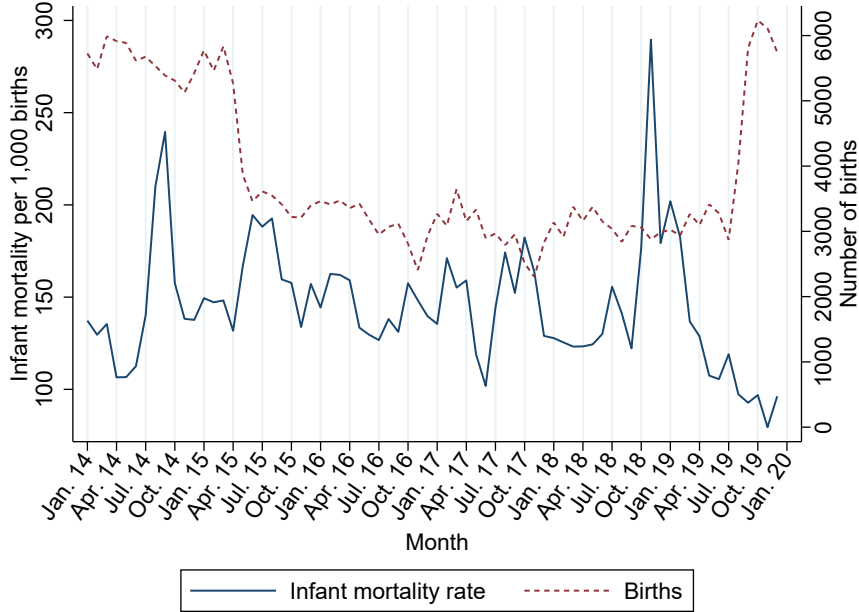


**Figure 2:** Monthly infant mortality rate and absolute number of births 1914–1919

*Notes:* The graph depicts monthly the infant mortality rate (solid line) and total births (dashed line) in the Kingdom of Württemberg for the years 1914–1919. The infant mortality rate is calculated as the number of deceased infants less than one year old per 1,000 births. Stillbirths are not included. *Source:* Statistisches Landesamt (1922). Author’s design.

than the total number of deaths in Figure 1, there are two distinct peaks in July and November 1918. These peaks in the infant mortality rate coincide with the first and second waves of the influenza pandemic. Additional data indicate an increase in the number of stillbirths during the second wave in October and November 1918 relative to the average number of stillbirths in the given months in 1914–1917 by about 9.2 and 6.8 percent, respectively. The statistics thus provide some evidence that the 1918 influenza increased the risk of miscarriage (Bloom-Feshbach et al., 2011; Reid, 2005).

Figure 2 reveals two additional findings. First, a decline in the number of births in May 1915, i.e., ten months after the German Empire entered the war, the number of births decreased by 26.5 percent compared to the previous month and 34.3 percent compared to May 1914. During the war, the number of births remained at a low level and only reached pre-war levels in September 1919. Second, there is a peak in the infant mortality rate in August and September 1914. On average, 812 infants below the age of one died per month in 1914. In August and September 1914, however, 1,162 and 1,291 infants died, respectively. Such strong increases in infant mortality during the summer months were not uncommon and often caused by heatwaves. This illustrates that the relatively high volatility in the infant mortality rate is partially driven by shocks that are uncorrelated to the 1918 influenza pandemic, like heat waves, local epidemics, or changes in fertility. The more noise measure might complicate the estimation of the effect of income and pollution on the infant mortality rate by inflating standard errors (see Section 5).

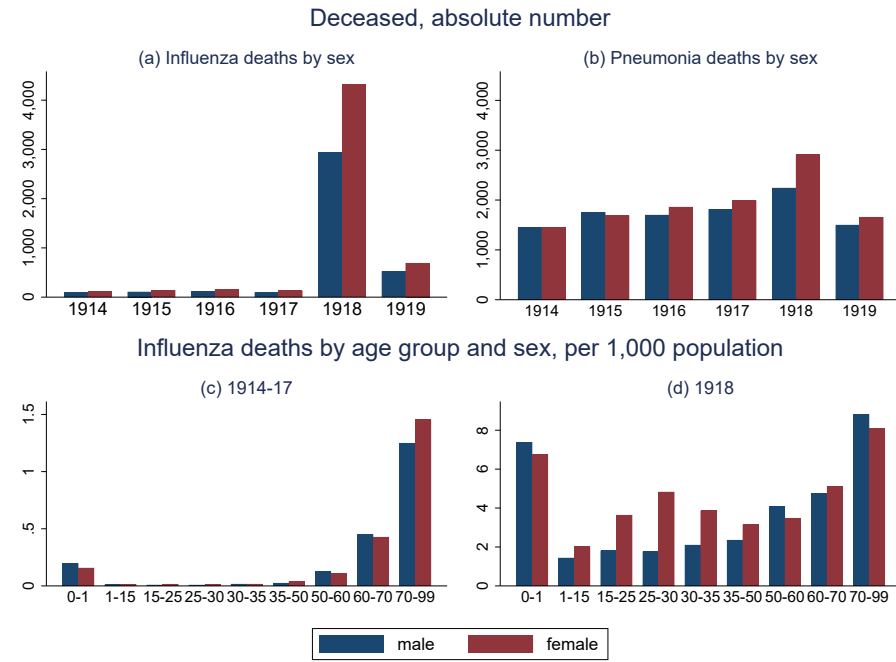


**Figure 3:** Aggregated influenza and pneumonia statistics for Württemberg

*Notes:* Figures 3 (a) and (b) show annual influenza and pneumonia deaths by sex for the years 1914 to 1919. Figure 3 (c) depicts the annual influenza mortality rate by age group averaged over the years 1914–1917 and Figure 3 (d) shows the influenza mortality rate by age group in 1918. The number of deceased does not include military personnel and stillbirths. *Source:* Statistisches Landesamt (1922). Author’s design.

The monthly data on all-cause mortality allow us to identify the onset of the 1918–1919 influenza pandemic and to distinguish the severity of the different waves in line with previous studies. Unfortunately, these data do not allow a further breakdown by cause of death, age, or sex. Therefore, I revert to annual data published in Statistisches Landesamt (1922). Figure 3 shows several annual mortality statistics by sex and age groups for the Kingdom of Württemberg, excluding military personnel and stillbirths. Figure 3 (a) shows the total number of all age influenza deaths per year and distinguishes between male (blue bars) and female (red bars) deaths. In the years 1914 to 1917, the statistics report on average 103 male and 134 female deaths per year due to influenza in Württemberg. This number increases sharply in 1918 to 2,941 male and 4,322 female deaths. Thus, the statistics indicate 7,026 excess influenza deaths in 1918, i.e., relative to the average of 1914–1917. In 1919, when the third wave of the 1918–1919 influenza pandemic hit Württemberg, the official statistics record 525 male and 692 female influenza deaths.

The influenza mortality statistics might suffer from under-reporting, especially due to cases of influenza that were wrongly assigned to pneumonia.<sup>13</sup> To evaluate the magnitude of this misreporting, Figure 3 (b) shows the annual number of pneumonia deaths by sex for the years 1914 to 1919. Indeed, there is an increase in reported pneumonia deaths in 1918 relative to

<sup>13</sup>Additionally, pneumonia was often caused by an initial influenza infection. Thus, although pneumonia might have been correctly diagnosed, some cases were caused by the influenza pandemic.

the previous years. In 1918 there are 2,242 male and 2,914 female deaths assigned to pneumonia, while the average for 1914–1917 is 1,679 and 1,747, respectively. This provides suggestive evidence that a considerable amount of influenza deaths have been assigned to pneumonia.<sup>14</sup> Therefore, most studies focus on all-cause mortality to prevent measurement error.

The reported differences in male and female influenza and pneumonia deaths should not be mistaken as differences in influenza mortality rates by sex. They are mainly driven by the exclusion of military personnel. When influenza and pneumonia deaths of military personnel are included, the differences between the sexes decrease significantly (see Figures A-4 (a) and (b) in the Appendix).

Figures 3 (c) and (d) report the influenza mortality rate per 1,000 population by nine age groups and sex. Figure 3 (c) shows the average mortality rates for the years 1914–1917, while Figure 3 (d) shows the influenza mortality rates for 1918. Unfortunately, there is no age distribution of the whole population available for each year. Thus, I use the age distribution of the latest census in 1910 to calculate the age-group-specific influenza mortality rates for each year. Given the decline in birth rates during WWI, the mortality rate of infants and the youngest age group are therefore downward biased.

The average influenza mortality rate per 1,000 population for the years 1914–1917 is 0.2 for infants, almost zero for the age groups between 1 and 50 years old, and increases significantly for people above age 50. The highest mortality rate is observed for the population above age 70, with 1.4 influenza deaths per 1,000 population. The average influenza mortality rate per 1,000 population in 1918 is about 3.0 and thus much higher than in the previous years.<sup>15</sup> The highest influenza mortality rates in Figure 3 (d) are observed for infants (7.4 for males and 6.7 for females) and people above age 70 (8.8 for males and 8.1 for females). The true infant mortality rate in 1918 is even higher because Figure 3 (d) neglects the decline in birth rates during WWI. Dividing the total number of influenza deaths of infants below the age of one by the number of births in 1917 increases the influenza mortality rate to 11.4. The age-specific distribution of influenza mortality in 1918 is commonly described as W-shaped, i.e., high mortality rates among the youngest and oldest population groups, but also relatively high mortality rates among young adults, peaking at about age 27 (Taubenberger et al., 2019).<sup>16</sup> Figure 3 (d) matches the W-

---

<sup>14</sup>Figures A-4 (c) and (d) in the Appendix show pneumonia mortality rates per 1,000 population by age groups and sex, for the years 1914–1917 and 1918, respectively. The increase in mortality rates specifically among young adults in 1918, in line with the W-shaped age-specific mortality pattern of the “Spanish Flu”, provides further evidence for the false assignment of cases.

<sup>15</sup>This is a lower bound of the true influenza mortality rate in 1918 because it neglects the influenza deaths among military personnel and does not account for wrongly assigned pneumonia deaths. On the other hand, it uses the population of the 1910 census as denominator, which causes an upward bias in the mortality rate. When I use the average total population of 1918 as denominator (Statistisches Landesamt, 1928), include influenza deaths among military personnel and excess pneumonia deaths in 1918 (Statistisches Landesamt, 1922), the adjusted influenza mortality rate per 1,000 population increases to 4.2.

<sup>16</sup>Figure A-5 in the Appendix documents a similar age-specific mortality pattern for Germany and its states.

shaped mortality pattern, but only for females. Again, this is due to the exclusion of influenza deaths of military personnel.

In general, the cause-specific mortality statistics describe a pattern of the “Spanish Flu” in Württemberg that is in line with the findings for other countries and regions. Yet, the data also demonstrate the difficulties to account for changes in birth rates, influenza mortality of military personnel, and insufficient diagnostics at the time. Therefore, most scholars use all-cause mortality to calculate excess mortality during the 1918–1919 influenza pandemic. However, the estimates for the excess mortality in Germany vary considerably. Johnson and Mueller (2002) estimate the death toll of the influenza pandemic in Germany to be about 225,000 and the excess mortality per 1,000 population to be 3.8. Patterson and Pyle (1991) estimate a range of 4.2 to 5. Ansart et al. (2009) use monthly all-cause mortality statistics and estimate the cumulative excess mortality rate to be 7.3. Murray et al. (2006) and Barro et al. (2020) compare the annual all-cause and influenza-related mortality in 1918–1920 with the average in the three-year periods before and after 1918–1920. The resulting cumulative excess mortality rates are 7.6 and 7.8, respectively. Thus, the estimates for Germany range from 3.8 to 7.8, i.e., they vary by a factor of about two. The variation in the estimates can be explained by different data sets, estimation methods, and definitions.

Applying the different approaches to the data available for Württemberg, the excess mortality rate per 1,000 population is 3.8 based on the estimation method in Ansart et al. (2009), 2.3 using all-cause mortality, and 3.9 using all influenza-related deaths based on the definitions by Murray et al. (2006) and Barro et al. (2020), respectively.<sup>17</sup> In addition, I re-estimate excess mortality rates for Germany and its states using mortality and population statistics published in Statistisches Reichsamt (1920, 1921a, 1922, 1924, 1925), see Appendix A.3 for further details. The estimates for Württemberg are slightly higher, with 2.5 and 4.0 excess deaths per 1,000 population based on the definitions by Murray et al. (2006) and Barro et al. (2020). For Germany, the respective estimates are 5.4 and 5.9 excess deaths per 1,000 population, with a range of 2.5–8.0 and 4.0–7.3 across the German states, see Table A-2 in the Appendix. Thus, the estimates for Württemberg are at the lower end of the estimates for Germany.

The variation in regional excess mortality rates raises the question of underlying factors. In the contemporary public perception, there was a link between influenza mortality, food shortages, and the poor health situation caused by the war (Michels, 2010). On the other hand, the relatively high mortality rate observed among healthy young adults seemingly contradicts this explanation (Bogusat, 1923; Taubenberger et al., 2019). Bootsma and Ferguson (2007) show the effectiveness of non-pharmaceutical interventions (NPIs) on pandemic mortality in US

---

The W-shaped curve of age-specific influenza mortality, however, is not always observed (Cilek et al., 2018).

<sup>17</sup>Further details on the estimation strategies and results are presented in the Appendix A.3. Unfortunately, I could not determine the exact definitions used by (Johnson and Mueller, 2002) and (Patterson and Pyle, 1991).

cities. These measures included the closure of schools and churches or mandated mask-wearing. However, NPIs can not explain regional differences in Germany because stringent measures were rarely introduced or were short-lived (Witte, 2003; Michels, 2010).

Furthermore, previous studies have discussed the effect of income and air pollution on regional differences in pandemic severity. Figure 4 shows that both factors correlate with excess mortality rates of German states and Prussian provinces.<sup>18</sup> Univariate linear regressions indicate a positive and statistically significant association between influenza-related excess mortality rates and GDP per capita in 1907 (0.004, s.e. 0.002) and installed coal-fired capacity in 1913 (0.069, s.e. 0.020). However, in a regression with both factors, the association between income and excess mortality becomes negative (-0.005, s.e. 0.003), while the pollution effect remains positive and statistically significant (0.111, s.e. 0.035). These results motivate a further analysis of the two factors.

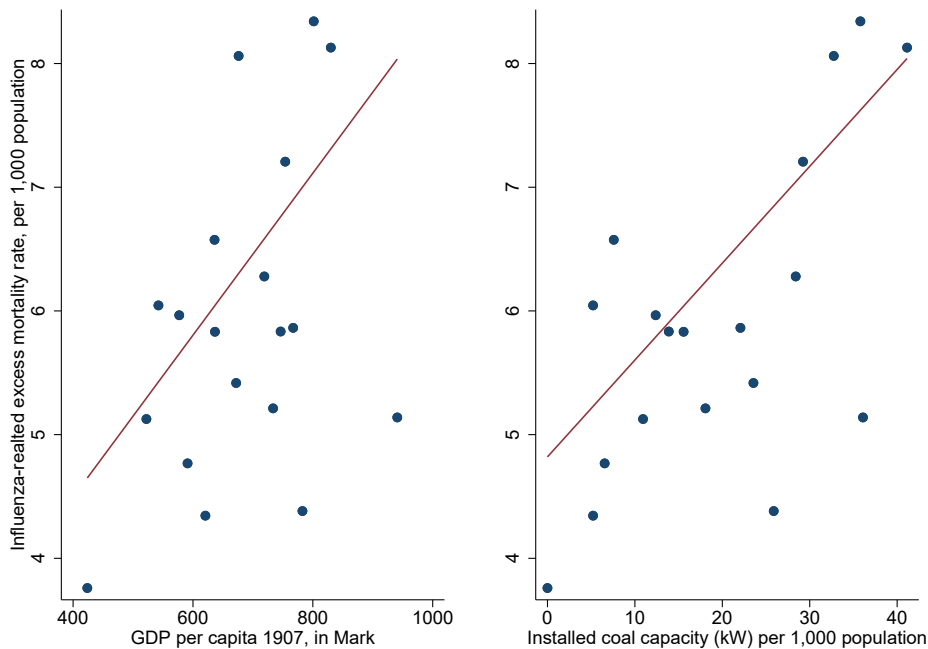


**Figure 4:** Association of income and pollution with influenza-related excess mortality 1918–20 for German states and Prussian provinces

*Notes:* The graph shows the association of income (left panel) and pollution (right panel) with influenza-related excess mortality 1918–20 for German states and Prussian provinces. The influenza related mortality rate per 1,000 population, includes all deaths from influenza, pneumonia, other diseases of the respiratory organs, tuberculosis, and whooping cough. The excess mortality rate is the sum of deviations in 1918–20 from the average in 1921–23. The income level is measured by GDP per capita in 1907. Pollution is calculated as the installed coal-fired capacity 1913 in kW per 1,000 population. *Sources:* Herzig et al. (2017), Frank (1993), and Statistisches Reichsamt (1920, 1921a, 1922, 1924, 1925), see Appendix A.3 for further details. Author’s design.

<sup>18</sup>Data for the states Mecklenburg-Schwerin and Mecklenburg-Strelitz are missing. Furthermore, Berlin is excluded from the analysis because it was the only metropolis of Germany and had significantly different characteristics. However, the results hold qualitatively if Berlin is included (see Figure A-6 in the Appendix).

### 3 Data

The remainder of the paper focuses on the effect of income and air pollution on pandemic mortality rates during the 1918 influenza pandemic. For the estimations, I use digitized annual data on vital statistics (all-age and infant all-cause mortality, number of births) for the universe of parishes in Württemberg in 1914–1925 (Staatsarchiv Ludwigsburg E 258 VII Bü 120 and 122). I aggregate parishes to take border changes during the sample period into account.<sup>19</sup> Unfortunately, the vital statistics on the parish level are missing for the county *Hall* and two parishes. Thus, there are 1,763 parishes in the resulting data set. The median parish has a land area of 8.7 square kilometers and 649 inhabitants in 1910.

I combine these data with rich socio-economic data from various population and occupation censuses, digitized by Braun and Franke (2019). In particular, the population data are based on censuses in 1910, 1919, and 1925 (Statistisches Landesamt Baden-Württemberg, 2008). To get annual population figures for each parish, I linearly interpolate the population between census years.<sup>20</sup> Based on the annual vital statistics and interpolated population data, I calculate the annual all-cause mortality rate per 1,000 population and the annual infant mortality rate per 1,000 births (*IMR*). To prevent biased estimates due to the large changes in fertility during WWI, I subtract the number of infants deceased at age one and below from the total number of deaths. Thus, the main dependent variable is defined as the number of deaths above the age of one per 1,000 population, excluding deaths among military personnel and stillbirths.<sup>21</sup> Henceforth, I will refer to this variable as mortality rate (*MR*) if not otherwise stated.

The two explanatory variables of interest are the parish income and air pollution levels. Income per capita is measured as the total taxable income of natural persons in 1907, i.e., income net of tax allowances and other deductions, divided by total population (Königliches Statistisches Landesamt, 1910).<sup>22</sup> To measure pollution, I link the data with available information on the location of coal-fired power plants, a major source of air pollution in the early 20th century (Clay et al., 2018).<sup>23</sup> The location of power plants in 1914 is taken from a map by Ott et al. (1981). The map includes all 594 power plants in Württemberg and neighboring Baden and

---

<sup>19</sup>Figure A-7 in the Appendix shows parish borders. We digitized parish borders from Kommission für geschichtliche Landeskunde in Baden-Württemberg and Landesvermessungsamt Baden-Württemberg (1972) and used information on border changes from Statistisches Landesamt Baden-Württemberg (2008).

<sup>20</sup>Alternatively, I project the population for each parish based on the annual number of births and deaths and only interpolate the residual that is due to migration. The estimation results using this alternative population measure are virtually identical. The results are not reported for the sake of brevity but can be received on request.

<sup>21</sup>The main results are, however, robust to the inclusion of infant mortality, see Section 5.2.

<sup>22</sup>Parish-level income data are not available for later years. However, per capita income in 1907 and 1917 are highly correlated at the county level (correlation coefficient of 0.905, rank correlation coefficient of 0.790).

<sup>23</sup>Data on actual air pollution are not available for Württemberg in the early 20th century. However, the usage of coal was the main driver of pollution during this period (Bailey et al., 2018; Beach and Hanlon, 2017). Therefore, and under the assumption that the use of coal in electric power plants is correlated with the total use of coal—both driven by the energy demand and the relative price of coal-generated energy—the installed coal-fired power plant capacity is used to proxy air pollution.

Hohenzollern. I geo-referenced the map using geographic information software to get the location of each power plant. In addition, the map provides information on the type of power generation and the installed maximum capacity. For each parish, I calculate the installed steam-powered capacity (*Dampfkraft*) in MW within 50 kilometers.<sup>24</sup>

For the later estimation, I generate dummies for the terciles of income 1907. Hence, these dummies indicate parishes in the sample with low, medium, and high average income. Independently, I generate dummies for the terciles of installed coal-fired power plant capacity within 50 kilometers. The average income per capita is 320.7 *Mark* (see Table 1). However, low-income parishes have an average income of 226.0 *Mark* per capita. The average income increases to 312.6 and 423.6 *Mark* per capita for medium and high-income parishes. The average installed coal-fired power plant capacity within 50 kilometers is 2.3 MW, 19.2 MW, and 53.7 MW for the low, medium, and high tercile. The average over all parishes is 24.9 MW.

Column (1) of Table 1 summarizes the mean and standard deviation of the main variables in the data set. The average mortality rate in 1914–1925 is 11.8 deaths per 1,000 population, with a standard deviation of 5.8. The average infant mortality rate in Württemberg is 135.4 per 1,000 births, with a standard deviation of 139.9.<sup>25</sup> Columns (2) and (3) show the mean difference in mortality rates between low-income parishes and medium and high-income parishes, respectively. In parishes with a medium-income, there are on average 0.5 fewer deaths per 1,000 population compared to parishes in the low-income tercile. The difference is statistically significant at the one percent level (s.e. 0.098). Also, parishes in the high-income tercile have a significantly lower mortality rate. However, the mortality rates of the three groups evolve largely in parallel over time, as shown in Figure 5. The average infant mortality rate is significantly higher in medium and high-income parishes.<sup>26</sup>

Columns (4) and (5) of Table 1 show the average difference in (infant) mortality rates between parishes with low and medium and low and higher coal-fired capacity, respectively. There is no statistically significant difference in average mortality rates by coal-fired capacity. Moreover, Figure 6 shows that the average mortality rate of all three groups moves in parallel over the period 1914 to 1925 but in 1918. The infant mortality rate, however, is significantly lower in parishes with medium and high coal-fired capacity.<sup>27</sup>

---

<sup>24</sup>Clay et al. (2018, 2019) use a similar radius of 30 miles (approximately 48.3 kilometers). The radius is chosen because power plant emissions disperse locally and Levy et al. (2002) show that about 40 percent of primary fine particulate matter (PM<sub>2.5</sub>) exposure is located within 50 kilometers of modern coal-fired power plants. The dispersion radius, however, depends on the height of the smokestack, which was likely lower in early 20th century Württemberg. Thus, an even higher share of total exposure would have occurred within 50 kilometers. See also the discussion of dispersion models in Appendix Section A.4.

<sup>25</sup>The average infant mortality rate in Württemberg was relatively high compared to other Western European countries. For instance, the average infant mortality rate in the same period was 87.6 in England and Wales, 112.1 in France and 76.8 in the Netherlands (Rothenbacher, 2002).

<sup>26</sup>Figure A-8 in the Appendix shows the annual average infant mortality rate 1914–1925 by income tercile.

<sup>27</sup>Figure A-9 in the Appendix shows the annual average infant mortality rate 1914–1925 by coal capacity tercile.

**Table 1:** Descriptive statistics

	All	Income		Coal	
	(1)	Medium	High	Medium	High
	(1)	(2)	(3)	(4)	(5)
<i>Outcomes</i>					
MR per 1,000 pop. 1914-25	11.766 (5.774)	-0.536 [0.098]	-0.690 [0.100]	-0.123 [0.101]	-0.015 [0.098]
IMR per 1,000 births 1914-25	135.420 (139.857)	7.210 [2.359]	6.739 [2.405]	-17.933 [2.505]	-36.638 [2.225]
Excess MR per 1,000 pop. 1918	4.094 (6.455)	-1.729 [0.384]	-1.790 [0.388]	0.242 [0.387]	1.432 [0.367]
Excess IMR per 1,000 births 1918	20.022 (174.892)	-10.234 [10.597]	8.162 [10.898]	-10.456 [11.359]	-26.015 [8.849]
<i>Explanatory variables</i>					
Tax income per capita 1907 ( <i>Mark</i> )	320.683 (97.176)	86.794 [1.842]	198.074 [3.759]	-44.427 [5.163]	-59.682 [5.582]
Coal capacity within 50 km (MW)	24.911 (23.130)	-8.345 [1.326]	-15.071 [1.286]	16.869 [0.576]	51.341 [0.219]
<i>Controls</i>					
Pop. 1910 (log)	6.556 (0.853)	0.179 [0.038]	0.343 [0.053]	-0.006 [0.047]	0.374 [0.049]
Pop. density 1910 (log)	4.412 (0.663)	-0.091 [0.032]	-0.059 [0.041]	0.160 [0.033]	0.727 [0.034]
Industry employment share 1905	11.071 (7.529)	2.462 [0.365]	3.743 [0.443]	1.839 [0.400]	4.735 [0.411]
Establishment size 1895 (log)	1.731 (1.065)	0.161 [0.043]	0.603 [0.068]	-0.028 [0.049]	0.168 [0.065]
Hydro capacity within 50 km (MW)	22.441 (15.044)	-6.514 [0.909]	-11.275 [0.830]	14.181 [0.716]	16.874 [0.639]
Birth non local 1900 (%)	0.262 (0.116)	0.028 [0.006]	0.124 [0.006]	-0.080 [0.007]	-0.091 [0.006]
Railway station 1910, dummy	0.279 (0.448)	0.105 [0.024]	0.247 [0.025]	0.004 [0.025]	0.078 [0.026]
Road access 1848, dummy	0.483 (0.500)	0.087 [0.029]	0.199 [0.029]	-0.117 [0.029]	-0.040 [0.029]
River access, dummy	0.078 (0.268)	0.067 [0.013]	0.095 [0.015]	-0.025 [0.015]	-0.007 [0.016]
Dist. to military base 1918 (km)	5.607 (3.412)	-0.086 [0.182]	-0.566 [0.201]	-1.069 [0.209]	-2.629 [0.188]

*Notes:* The table shows average values and associated standard deviations in parenthesis below for all 1,763 parishes in the data set (Column (1)). In Columns (2) to (5), the table shows mean differences between parishes with lowest income per capita in 1907 (Columns (2) and (3)) and lowest installed coal-fired power plant capacity within 50 kilometers (Columns (4) and (5)), relative to medium (Columns (2) and (4)) and high levels (Columns (3) and (5)). The standard errors of a two-sided mean difference t-test are in brackets below.

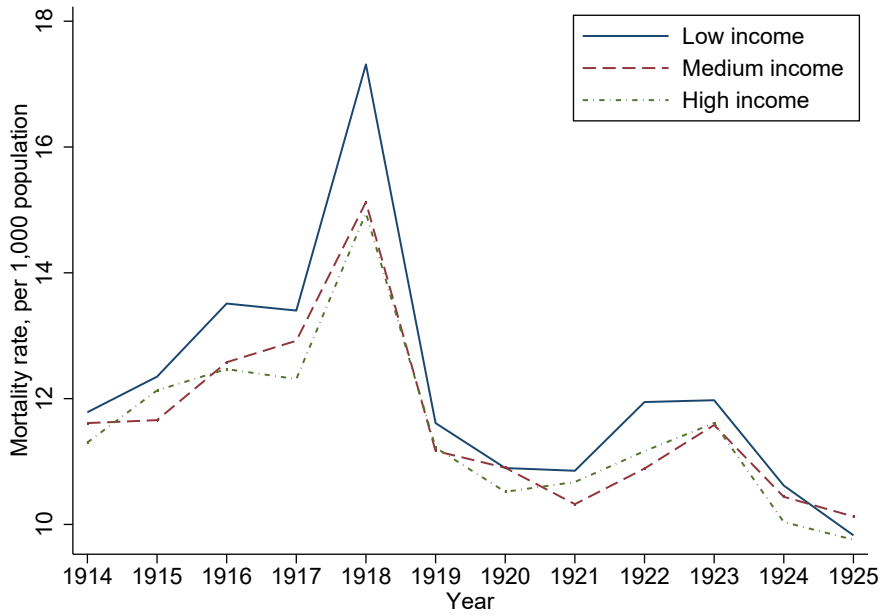


**Figure 5:** Mortality rate 1914–1925 by income tertile

*Notes:* The figure shows the annual average mortality rate per 1,000 population in parishes for the years 1914 to 1925 by tertiles of income 1907. *Sources:* Königliches Statistisches Landesamt (1910), Statistisches Landesamt Baden-Württemberg (2008), and Staatsarchiv Ludwigsburg E 258 VII Bü 120. Author's design.

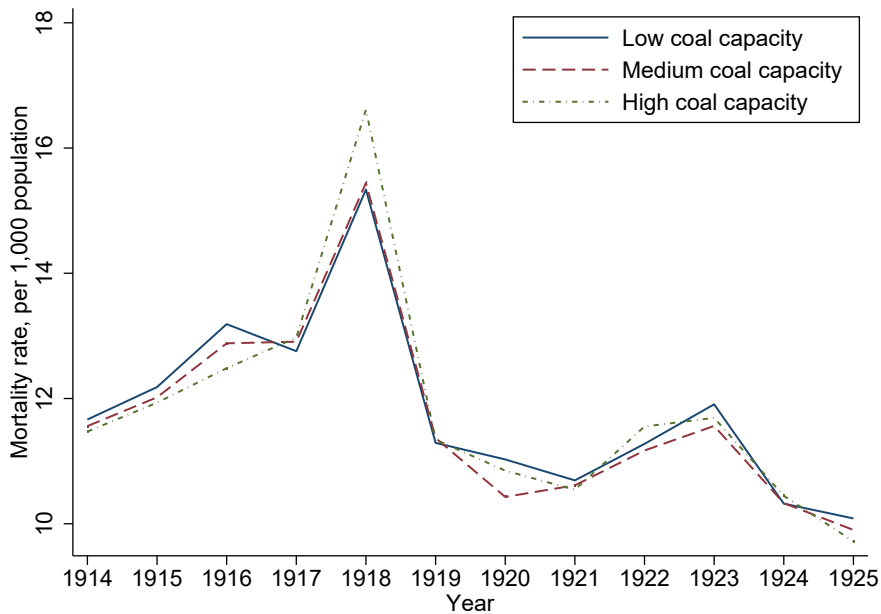


**Figure 6:** Mortality rate 1914–1925 by coal capacity tertile

*Notes:* The figure shows the annual average mortality rate per 1,000 population in parishes for the years 1914 to 1925 by tertiles of installed coal-fired power plant capacity within 50 kilometers. *Source:* Ott et al. (1981), Statistisches Landesamt Baden-Württemberg (2008), and Staatsarchiv Ludwigsburg E 258 VII Bü 120. Author's design.

Table 1 also shows the excess mortality rate in 1918. The excess mortality rate for parish  $i$  is the difference between the observed mortality rate in 1918 and the predicted mortality rate. The prediction for 1918 is based on a model with parish fixed effects and parish-specific linear trends, estimated for the sample period 1914–1917, 1919–1925 as in Clay et al. (2019). Figure A-7 in the Appendix illustrates the variation of excess mortality rates across parishes. The figure also shows that there is no clear spatial pattern of excess mortality in Württemberg. The excess infant mortality rate is calculated analogously. The average excess mortality rate in 1918 is 4.1 deaths per 1,000 population. The magnitude of this estimate is thus comparable to the estimates presented in Section 2.

The differences in Columns (2) to (5) provide first unconditional evidence of the effect of income and pollution on excess mortality during the 1918 influenza pandemic. Medium and high-income parishes had significantly lower excess mortality rates in 1918. Compared to low-income parishes, the excess mortality rate decreases by 1.7 and 1.8 excess deaths per 1,000 population. Parishes with the highest coal-fired capacity have 1.4 additional excess deaths per 1,000 population. The difference is statistically significant at the one percent level (s.e. 0.367). For the excess infant mortality rate, the differences are not statistically significant except for highly polluted parishes. The unconditional difference is negative, which would imply that the excess infant mortality rate is significantly lower in parishes with high coal-fired capacity compared to parishes with low coal-fired capacity.

The control variables are log population, log population density in 1910, and the ratio of industrial employment over 100 population in 1905, based on the occupation census 1907 (Königliches Statistisches Landesamt, 1910). The occupation census comprises parish-level information on the number of full-time gainfully employed persons (self-employed and dependent) in agriculture, industry, and trade and transport. Furthermore, I use data from the *Gewerbestatistik* to calculate the establishment size in industry as the average number of persons employed in an establishment (*Hauptbetrieb*) in 1895 (Königliches Statistisches Landesamt, 1900), the installed capacity of hydroelectric power plants within 50 kilometers (Ott et al., 1981), and the population share that is born in another parish in the year 1900 (Statistisches Landesamt Baden-Württemberg, 2008). To control for access to transport infrastructure, I include binary dummy variables that indicate a railway station in the parish in 1910 (Königliches Statistisches Landesamt, 1911), access to a river navigable in 1845, and connection to a paved road in 1848 (Kunz and Zipf, 2008). Finally, I digitized the location of each military base in Württemberg in 1918 and calculated the distance to the nearest military base in kilometers (von Moser, 1927).

Table 1 shows descriptive statistics for the control variables. Parishes with higher income have a higher population size, are more industrialized, with on average larger establishments, and have better access to transport infrastructure. At the same time, parishes with high coal-

fired capacity are larger, more densely populated, and more industrialized. Moreover, they have more hydroelectric capacity installed within 50 kilometers and are further away from the nearest military base. Overall, the control variables capture significant differences between parishes by income and pollution level.

## 4 Estimation strategy

The empirical analysis is based on a difference-in-differences approach that compares the average change in mortality rates during the influenza pandemic across parishes with high and medium-income (coal-fired capacity) relative to parishes with low-income (coal-fired capacity).<sup>28</sup> The baseline empirical model is specified by the following equation

$$MR_{it} = \sum_{t=1914}^{1925} \beta_{1t} MI_i \cdot d_t + \sum_{t=1914}^{1925} \beta_{2t} HI_i \cdot d_t + \sum_{t=1914}^{1925} \beta_{3t} MP_i \cdot d_t + \sum_{t=1914}^{1925} \beta_{4t} HP_i \cdot d_t + \sum_{t=1914}^{1925} \gamma_t \overline{MR}_{i,1910-13} \cdot d_t + \delta X_i \cdot I_{\{1918\}} + d_i + d_t + d_{kt} + \varepsilon_{it}, \quad (1)$$

where  $MR_{it}$  is the mortality rate in parish  $i$  and year  $t$ , defined as the number of deaths, excluding infants less than one year old, stillborn children, and military personnel. The mortality rate is regressed on binary dummy variables that indicate parishes with medium income  $MI_i$  and coal-fired capacity  $MP_i$ , and high-income  $HI_i$  and coal-fired capacity  $HP_i$ , each interacted with a set of time fixed effects  $d_t$ . The coefficients  $\beta_{jt}$  are normalized, such that  $\beta_{j,1917} = 0$ . Thus, the estimator  $\beta_{1t}$  captures the differential change in the mortality rate from 1917 to year  $t$  in medium-income parishes relative to the change in low-income parishes, conditional on pre-pandemic characteristics.<sup>29</sup>

To control for pre-pandemic parish characteristics, equation (1) includes several control variables. Among these control variables are the average mortality rate of the years 1910–1913 in parish  $i$  ( $\overline{MR}_{i,1910-13}$ ), interacted with a set of time fixed effects  $d_t$  and a set of time-invariant parish specific controls variables  $X_i$  that are interacted with an indicator variable  $I_{\{1918\}}$ . The indicator variable  $I_{\{1918\}}$  is one for the pandemic year 1918 and zero otherwise. Furthermore, equation (1) includes parish fixed effects  $d_i$  that control for any time-invariant parish characteristics, e.g., geographic factors. The time fixed effects  $d_t$  and district times year fixed effects  $d_{kt}$  control for influences on mortality that vary by time and district, like local weather shocks. The standard errors  $\varepsilon_{it}$  are clustered at the county level.

The control variables in  $X_i$  are as specified in Table 1 and can broadly be grouped into two

<sup>28</sup>The empirical strategy is similar to the approach used in Hornbeck (2012) and Clay et al. (2018).

<sup>29</sup>The results are robust to changes in the baseline year, see also Section 5.2.

categories. The first category comprises variables that control for socio-economic development and related pre-pandemic health differences between parishes. Population size and density, industry employment share, firm size, installed hydroelectric capacity, and the share of non-local born inhabitants can be grouped into this first category. Population size and density are included because there is empirical evidence that larger cities in the US might have been able to implement more effective non-pharmaceutical interventions or had a higher immunity in the second wave due to an earlier exposure to the virus (Bootsma and Ferguson, 2007; Acuna-Soto et al., 2011; Clay et al., 2019). On the other hand, densely populated areas could have enhanced the spread (Mills et al., 2004; Chowell et al., 2007). The transmission of the virus might have been also higher if people had more contact in their workplace. Therefore I control for the average firm size.

Several studies document the effect of pre-pandemic health on pandemic mortality (Bootsma and Ferguson, 2007; Clay et al., 2019). Here, I include the average mortality rate in 1910–1913 and the share of population born outside of the parish to control for this effect (Clay et al., 2018, 2019). A higher average mortality rate in 1910–1913 indicates a poorer local health environment or a different age structure of the population or both. The share of the non-local-born population takes into account that during the industrialization, rural flight brought many workers into the economic centers. These (internal) migrants are probably younger, poorer, and have worse health than the average local population.<sup>30</sup> The inclusion of the industrial employment share and firm size controls for adverse health outcomes of industrial employment caused by the relatively low level of occupational safety.

The second category of control variables captures the potential difference in the exposure to the virus and the timing of onset. Parishes with better access to transport infrastructure might have been more exposed to the virus and might have had an earlier onset (Hogbin, 1985). However, the direction of this effect on pandemic mortality is unclear. An earlier onset of the pandemic might have increased mortality because the virulence may have declined over time (Clay et al., 2019).<sup>31</sup> At the same time, more central parishes might have seen a stronger first wave and thus had a higher immunity in the second, more deadly wave (Acuna-Soto et al., 2011; Clay et al., 2019). On the other hand, very remote parishes might have even escaped the pandemic (Erkoreka, 2020). Therefore, I include binary indicators that control for access to the railway, central roads, and navigable waterways. I also control for the distance to the nearest

---

<sup>30</sup>Table 1 shows that the average mortality rate is lower in parishes with higher income, but there is no significant difference in average mortality rates between parishes by pollution tercile. Thus, one channel of the income effect could be the effect on pre-pandemic health differences, if the model does not capture the pre-pandemic health sufficiently. Likewise, the estimator of the pollution effect would be upward biased, if less healthy individuals sorted into highly polluted parishes and the pre-pandemic health differences are not captured by the model in equation (1). The insignificant differences in the average mortality rate, however, do not indicate such a selective migration pattern.

<sup>31</sup>The higher case fatality rates in the second wave could have been due to an increased frequency of secondary bacterial pneumonia rather than an increased virulence of the influenza virus (Taubenberger et al., 2019).

military base because the spread of the virus was likely accelerated by the movement of troops (Patterson and Pyle, 1991).

For a causal interpretation of the effect of income and coal capacity, it must hold that, conditional on control variables, the expected change in pandemic mortality rates would have been the same across parishes with low, medium, and high-income (coal capacity) in the absence of the difference in income (coal capacity). In terms of the difference-in-differences model, this assumption is referred to as common trend assumption. It must also hold that there is no unobservable factor that influences mortality and correlates with income and coal capacity. Since I control for parish fixed effects, time fixed effects, and time times district fixed effects, these unobservable factors would also need to vary over time at the sub-district level to bias the estimates.

## 5 Results

This section presents the paper’s main results on the effect of income and pollution on mortality rates during the 1918 influenza pandemic in Württemberg. In addition to the parish level estimates, the section discusses several robustness checks and presents estimates with data aggregated at the county level.

### 5.1 Parish level estimates

Figure 7 shows the differential changes in average mortality rates between middle and low-income parishes (left panel) and high and low-income parishes (right panel) from 1914 to 1925, relative to the baseline year 1917. The results are based on a reduced version of equation (1), excluding the indicators for pollution, the control variables in  $X_i$ , and county times year fixed effects.<sup>32</sup> The vertical bars in Figure 7 indicate 95 percent confidence intervals. The pandemic year 1918 is indicated by a vertical dashed line.

The change in the mortality rate 1918 in middle-income parishes relative to low-income parishes is significantly lower by -1.7 deaths per 1,000 population. The same holds for high-income parishes with a point estimate of -1.3. Or in other words, the spike in 1918 mortality was particularly large in poor parishes.

Similarly, Figure 8 compares the changes in mortality between parishes in the low tercile of installed coal-fired capacity and parishes in the medium (left panel) and high tercile (right panel) from 1914 to 1925, relative to the baseline year 1917. The estimation is based on a reduced model as in Figure 7, but with indicators for medium and high coal capacity ( $MP_i$  and  $HP_i$ )

---

<sup>32</sup>Formally, this renders equation (1) to:  $MR_{it} = \beta'_{1t}MI_i \cdot d_t + \beta'_{2t}HI_i \cdot d_t + \gamma'_t\overline{MR}_{i,1910-13} \cdot d_t + d_i + d_t + \varepsilon_{it}$ .

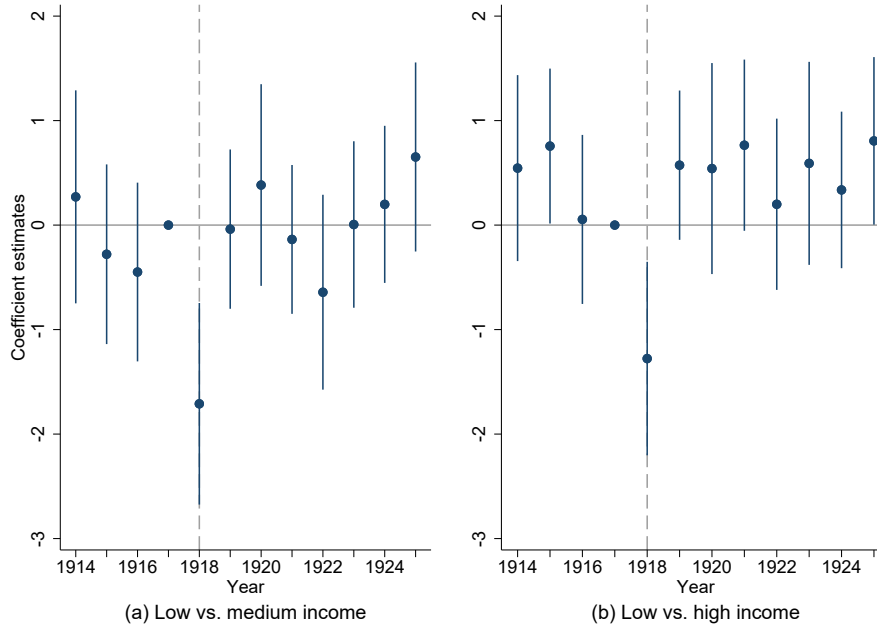


**Figure 7:** Estimated difference in mortality rate changes by income

*Notes:* The graph depicts differences in mortality rates between parishes with middle and low-income per capita levels (left panel) and the high and low-income per capita levels (right panel), as estimated in an event study regression. Differences are expressed relative to the baseline difference in 1917. Point estimates are marked by a dot. The vertical bands indicate the 95 percent confidence interval of each estimate. The red dashed vertical line indicates the pandemic year 1918. Author’s design.

instead of income indicators. There is no significant difference in the change in mortality rates in parishes with medium coal capacity compared to parishes with low coal capacity. Parishes with high levels of installed coal-fired capacity, on the other hand, have a significantly stronger increase in mortality rates. In these parishes, the mortality rate increases by an additional 1.1 deaths per 1,000 population. The effect is statistically significant at the five percent level.

Thus, Figures 7 and 8 indicate a lower mortality rate increase for parishes with higher incomes and less pollution between 1917 and 1918. Additionally, the figures show that the estimates for the pandemic year 1918 deviate strongly from all other years. There is no general difference in mortality rate changes that distinguish the different parish groups, other than in 1918. Indeed, only three out of the 44 reported estimates in Figures 7 and 8 are statistically significant at the five percent level (not counting the 1918 estimates), and all show the opposite sign.<sup>33</sup> Out of the 12 estimates for the pre-pandemic period, only two are statistically significant. These estimates provide suggestive evidence for the common trend assumption to hold, i.e., there is no systematic difference in mortality rate changes in non-pandemic years.

Table 2, Panel A, Columns (1) and (3) show the point estimates and standard errors for the interactions of medium and high-income and coal capacity indicators with the indicator for 1918.

<sup>33</sup>These estimates could indicate a negative effect of poverty and pollution during the harsh winter of 1916–1917. If the mortality rate in the reference year 1917 is higher in poor and highly polluted parishes this would downward bias the 1918 estimates.

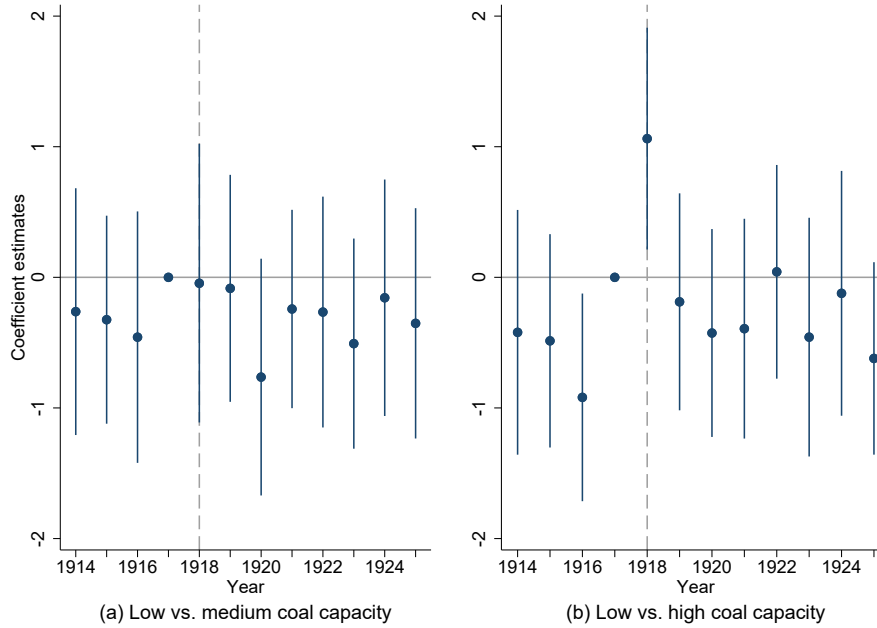


**Figure 8:** Estimated difference in mortality rate changes by coal capacity

*Notes:* The graph depicts differences in mortality rates between parishes with middle and low coal capacity levels (left panel) and high and low coal capacity levels (right panel), as estimated in an event study regression. Differences are expressed relative to the baseline difference in 1917. Point estimates are marked by a dot. The vertical bands indicate the 95 percent confidence interval of each estimate. The red dashed vertical line indicates the pandemic year 1918. Author's design.

The results correspond to the results in Figures 7 and 8. In low-income parishes, the mortality rate increased from 13.4 in 1917 to 17.3 in 1918, an increase of 3.9 deaths per 1,000 inhabitants or 29 percent. The point estimates in column (1) indicate that the respective increase in medium and high-income parishes was lower by 1.7 and 1.3 deaths per 1,000 population. Both estimates are statistically significant at the one percent level. In column (2), I include the full set of control variables as well as district times year fixed effects. The estimates for the income effect in column (2) are slightly lower but remain statistically and epidemiologically significant.

Table 2, column (3) shows the results for coal-fired capacity. In parishes with the highest installed coal capacity within 50 kilometers, the mortality rate increases by an additional 1.1 deaths per 1,000 population. The estimate is statistically significant at the five percent level, with a standard error of 0.425. The point estimate is virtually identical in column (4), where I include the full set of controls and district times year fixed effects. The change in mortality rates is almost identical for parishes with low and medium coal capacity, an average increase of about 2.6 deaths per 1,000 population between 1917 and 1918.

Column (5) includes the measures for income and coal capacity simultaneously, and column (6) adds the full set of control variables. Thus, the estimates in column (6) are based on the full model as specified in equation (1).<sup>34</sup> Conditional on pre-pandemic socio-economic characteristics

<sup>34</sup>Table A-4 in the Appendix shows the full set of results including control variables.

**Table 2:** Baseline results – DiD Estimates

	(1)	(2)	(3)	(4)	(5)	(6)
<b>Panel A:</b> Dependent variable: Mortality rate 1914–1925						
Income medium $\times$ 1918	-1.710*** (0.482)	-1.378*** (0.466)			-1.638*** (0.494)	-1.379*** (0.473)
Income high $\times$ 1918	-1.277*** (0.463)	-0.993* (0.526)			-1.147** (0.494)	-0.969* (0.526)
Coal medium $\times$ 1918			-0.045 (0.533)	-0.101 (0.597)	-0.320 (0.528)	-0.202 (0.590)
Coal high $\times$ 1918			1.062** (0.425)	1.056* (0.564)	0.715 (0.445)	0.958* (0.569)
Observations	21,156	21,156	21,156	21,156	21,156	21,156
<b>Panel B:</b> Dependent variable: Infant mortality rate 1914–1925						
Income medium $\times$ 1918	-18.254 (16.102)	-24.947 (17.079)			-19.678 (16.060)	-23.870 (16.930)
Income high $\times$ 1918	11.715 (15.283)	-5.478 (19.504)			8.881 (15.122)	-3.902 (19.028)
Coal medium $\times$ 1918			2.873 (16.273)	14.450 (17.268)	4.802 (16.398)	13.683 (17.468)
Coal high $\times$ 1918			-18.201 (14.607)	-9.434 (21.148)	-15.860 (14.944)	-9.741 (21.563)
Observations	21,097	21,097	21,097	21,097	21,097	21,097
FE	Yes	Yes	Yes	Yes	Yes	Yes
Year FE	Yes	Yes	Yes	Yes	Yes	Yes
Controls	No	Yes	No	Yes	No	Yes
Year $\times$ District FE	No	Yes	No	Yes	No	Yes

*Notes:* The table shows panel regression estimates of the effect of taxable income 1907 and installed coal-fired power plant capacity within 50 kilometers on the differential change in mortality rates (Panel A) and infant mortality rates (Panel B). Regressions (1) and (2) show the change in medium and high-income parishes between 1917 and 1918 relative to the change in low-income parishes. Regressions (3) and (4) show the change in medium and high coal capacity parishes between 1917 and 1918 relative to the change in low coal capacity parishes. Regressions (5) and (6) include income and coal capacity measures. All regressions include a full set of year and parish fixed effects. Regressions in Panel A include the average mortality rate 1910–1913 interacted with year fixed effects. Regressions in Panel B include the average infant mortality rate 1910–1913 interacted with year fixed effects. Columns (2), (4), and (6) include the full set of pre-treatment control variables  $X_i$  each interacted with an indicator variable for the year 1918 and year times district fixed effects. Standard errors clustered at the county level are in parentheses. \*\*\*, \*\*, and \* denote statistical significance at the 1, 5, and 10 percent level, respectively.

and the installed coal capacity, the change in the all-cause mortality is 1.4 less in medium relative to low-income parishes. Likewise, the average change in the mortality rate is lower by one death per 1,000 population for parishes in the high-income tercile compared to the low tercile. On the other hand, parishes with the highest level of installed coal-fired capacity had, on average, an additional increase by one death per 1,000 population. These effects are large compared to an average increase in the mortality rate between 1917 and 1918 of 2.9.

Table 2, Panel B, reports the results with the infant mortality rate, i.e., the number of infants deceased age one or below per 1,000 births, as the dependent variable. In contrast to the previous model, I now control for the average infant mortality rate 1910–1913 ( $\overline{IMR}_{i,1910-13}$ ) of parish  $i$ , instead of the average mortality rate 1910–1913 ( $\overline{MR}_{i,1910-13}$ ). All estimates are statistically insignificant. The results illustrate the difficulties in estimating the effect on infant mortality in the given sample. As discussed above, the infant mortality rate shows high variation and multiple shocks that are orthogonal to the influenza pandemic, e.g., heat waves or the response in fertility to WWI. Moreover, the relatively small unit of analysis, parishes with a median population of 649 inhabitants, causes random noise in the dependent variable and thus increases standard errors.

## 5.2 Robustness checks

In the previous estimations, I control for a variety of pre-pandemic factors. However, to address potential concerns that the results are driven by model specifications, characteristics of the sample, or the construction of variables, I perform several robustness checks in this section.

The power plant data also include information on power plants that use a mixture of coal, other fuels, and water power (*gemischter Antrieb*), and internal combustion engines (*Explosionsmotoren*). Thus, focusing on coal-fired power plants underestimates the pollution due to the generation of electric energy. This measurement error might attenuate the estimates of the pollution effect. Table 3 shows the results when these additional power plants are included. In Panel A, I measure the installed capacity as the sum of coal-fired capacity and the capacity of power plants that use a combination of coal and other sources of energy generation. The estimated effects are higher and statistically significant. The results of the full model in column (4) indicate that parishes in the high-capacity tercile had an additional increase of 1.7 deaths per 1,000 population compared to parishes in the low tercile. Panel B adds the capacity of power plants using internal combustion engines. Again, the results are higher than in the baseline specification and statistically significant. These results provide suggestive evidence that the previous results on the effect of pollution on pandemic mortality are a lower bound of the true effect.

**Table 3:** Robustness checks – Alternative pollution measures

	Mortality rate 1914–1925			
	(1)	(2)	(3)	(4)
<b>Panel A:</b> Capacity measure includes coal and power plants using a mix				
Income medium $\times$ 1918			-1.571***	-1.315***
			(0.500)	(0.476)
Income high $\times$ 1918			-1.017**	-0.870
			(0.500)	(0.536)
Capacity medium $\times$ 1918	0.279	0.487	0.084	0.408
	(0.552)	(0.546)	(0.553)	(0.556)
Capacity high $\times$ 1918	1.423***	1.785***	1.150**	1.709***
	(0.442)	(0.539)	(0.470)	(0.562)
<b>Panel B:</b> Capacity measure includes coal, mix, and combustion engines				
Income medium $\times$ 1918			-1.605***	-1.339***
			(0.502)	(0.478)
Income high $\times$ 1918			-1.087**	-0.922*
			(0.476)	(0.522)
Capacity medium $\times$ 1918	0.064	0.203	-0.179	0.103
	(0.520)	(0.494)	(0.494)	(0.499)
Capacity high $\times$ 1918	1.301***	1.584***	0.999**	1.500***
	(0.428)	(0.507)	(0.439)	(0.527)
Observations	21,156	21,156	21,156	21,156
FE	Yes	Yes	Yes	Yes
Year FE	Yes	Yes	Yes	Yes
Controls	No	Yes	No	Yes
Year $\times$ District FE	No	Yes	No	Yes

*Notes:* The table shows panel regression estimates of the effect of taxable income 1907 and installed power plant capacity within 50 kilometers on the differential change in mortality rates. In Panel A the power plants include coal-fired power plants and power plants that use a combination of coal and other means of power generation. Panel B adds the capacity of power plants that use combustion engines. Regressions (1) and (2) show the change in medium and high capacity parishes between 1917 and 1918 relative to the change in low capacity parishes. Regressions (3) and (4) include income and capacity measures. All regressions include a full set of year fixed effects, parish fixed effects, and the average mortality rate 1910–1913 interacted with year fixed effects. Columns (2) and (4) include the full set of pre-treatment control variables  $X_i$  each interacted with an indicator variable for the year 1918 and year times district fixed effects. Standard errors clustered at the county level are in parentheses. \*\*\*, \*\*, and \* denote statistical significance at the 1, 5, and 10 percent level, respectively.

Recent articles have used wind patterns to identify causal effects of air pollution on various outcomes, e.g., Beach and Hanlon (2017) on infant mortality. However, the dispersion of pollutants depends on the local wind patterns and topography. Appendix Section A.4 discusses the results of dispersion model simulations for Württemberg. A clear northeast drift of pollutants—as used in Beach and Hanlon (2017) for Britain—can not be found for Württemberg. However, the simulation results indicate a slight northern drift of pollutants. Table A-3 in the Appendix shows estimation results based on this dispersion pattern. Overall, the pollution effect estimates for high-capacity parishes are similar to the estimates in Table 2. In addition, the effect for medium-capacity parishes becomes positive and in the reduced model statistically significant at the 10 percent level. Nonetheless, the overall results are very similar to the baseline results.

The estimates in Table 2 show the differential change in mortality rates relative to the baseline year 1917. However, the virus that caused the influenza pandemic might have already spread before 1918 (Johnson, 2001; Taubenberger et al., 2019). Moreover, the mortality rate in 1917 was relatively high due to starvation and the harsh winter 1916–1917. If the mortality rate in 1917 is negatively correlated with income and positively correlated with coal-fired capacity, the estimates in Table 2 would represent a lower bound of the income and pollution effect on pandemic mortality.

Table A-5 in the Appendix presents results using 1914 as the baseline year instead of 1917. Therefore, the estimates in Table A-5 show the differential change in the mortality rate from 1914 to 1918 in medium and high-income (pollution) parishes relative to the change in low-income (pollution) parishes, conditional on pre-pandemic characteristics. The results of the full model in column (6) indicate that highly polluted parishes faced an additional increase of 1.3 deaths per 1,000 population (s.e. 0.623) relative to medium and low polluted parishes and that the increase in mortality rates was lower in medium and high-income parishes by 1.7 (s.e. 0.530) and 1.6 (s.e. 0.657) deaths per 1,000 population, relative to low-income parishes. In general, all point estimates (not including the medium coal capacity estimates) indicate a stronger effect and higher statistical significance levels than in Table 2. Thus, using 1917 as reference year might produce more conservative estimates.

The results in Table 2 hold qualitatively if I include infant deaths (see Appendix Table A-6), include World War I years only to account for any war-related parish specific fixed effects (Table A-7, Panel A), control for the annual number of deaths of military personnel at the parish level (Table A-7, Panel B),<sup>35</sup> include coal-fired power plants in Bavaria listed in Dettmar (1913) (Table A-8),<sup>36</sup> or allow the effect of each cross-sectional unit characteristic to vary by year as in

---

<sup>35</sup>I do not control for the number of military personnel deaths in the main specification because this variable could be considered a bad control. The variable includes deaths caused by the influenza pandemic, see Section 2, and therefore the conditions soldiers experienced at home, e.g., the exposure to pollution or low-income, could influence the mortality.

<sup>36</sup>Dettmar (1913) lists power plants in Germany and their characteristics. However, only a few coal-fired power

Hornbeck (2012) (Table A-9).

As a further robustness check, I replace the main explanatory variables with indicators based on income and coal-fired capacity quintiles (Table A-10). This addresses concerns that the results are driven by the specific division of the sample. The partition in quintiles shows the effect to be statistically insignificant for parishes with medium-high income compared to low-income parishes. However, the general results still indicate a negative income and a positive pollution effect on pandemic mortality. I also truncate the sample based on population size in 1910, i.e., I exclude the largest and smallest one (five) percent of parishes from the sample (Table A-11). The truncation reduces the average population size in the sample from 1,354.4 to 972.9 (809.4). The results of these robustness checks are in line with the baseline results. Thus, the effects are not driven by a significantly different health environment in the few urban centers or outliers in small villages' mortality rates. To account for spatial autocorrelation, I use Conley standard errors with cut-off distances of 10, 20, and 50 kilometers (Table A-12). Overall, the results remain statistically significant.

These alternative specifications confirm the positive effect of higher income levels and the negative effect of higher levels of coal-fired capacity on pandemic mortality rates.<sup>37</sup> Moreover, the results in Table 3 suggest that the pollution effect reported in Table 2 provides a lower bound for the actual effect of pollution on the pandemic mortality increase.

### 5.3 County-level estimates

An advantage of the data set is that it allows to exploit heterogeneity at the parish level. However, such detailed data are not always available. Often studies use more aggregated data at the county or even district level. Hence, existing heterogeneity within these larger areas could be averaged out and estimates biased towards zero. This problem is discussed as the modifiable areal unit problem in the literature (Fotheringham and Wong, 1991; Gotway and Young, 2002).

Figures 9 and 10 show the estimation results based on a reduced model as in Figures 7 and 8, respectively, but for data aggregated at the county level. The aggregated data set comprises 63 counties. In both figures, the estimated effect of income and coal-fired capacity shows the expected sign, i.e., a negative estimate for the relative change in mortality rates in 1918 compared to 1917 for medium and high-income counties compared to low-income counties and a positive estimate for counties with high compared to low levels of installed coal-fired capacity. However, none of these estimates is statistically significant. The statistical insignificance might just be a

---

near Württemberg are listed. Therefore, the average installed coal-fired capacity in the sample with Bavarian power plants increases only slightly from 24.911 to 24.958.

<sup>37</sup>The robustness checks have been also performed with the infant mortality rate as dependent variable. The results remain statistically insignificant and are not reported here. The results can be received upon request.

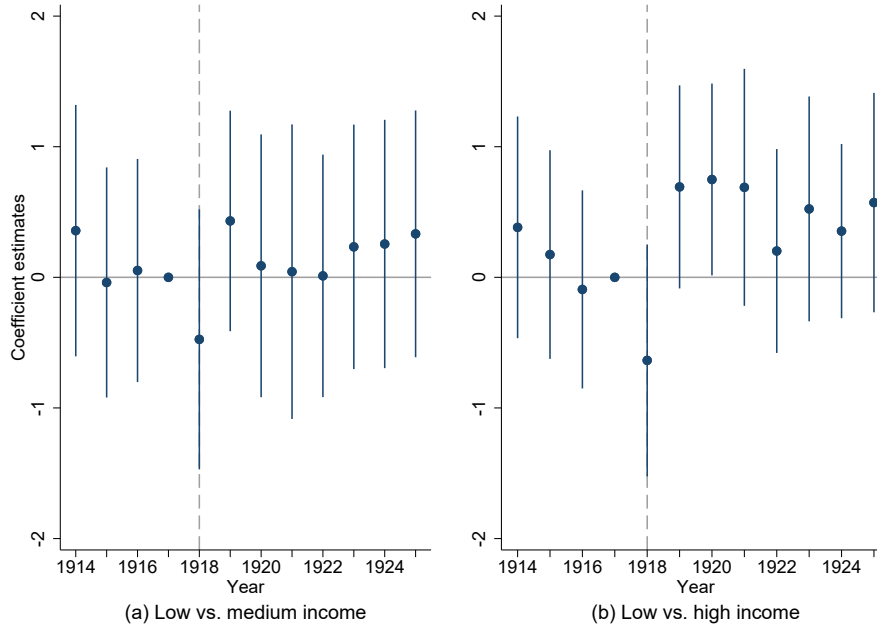


**Figure 9:** Estimated difference in mortality rate changes at the county level by income

*Notes:* The graph depicts differences in mortality rates between counties in the middle and low-income per capita tercile (left panel) and the high and low-income per capita tercile (right panel), as estimated in an event study regression. Differences are expressed relative to the baseline difference in 1917. Point estimates are marked by a dot. The vertical bands indicate the 95 percent confidence interval of each estimate. The red dashed vertical line indicates the pandemic year 1918. Author’s design.

result of the loss in statistical power due to the smaller sample size but also due to the aggregation itself. Therefore, the county-level estimates emphasize the importance of complementing existing studies at the aggregate level with analyses using more finely grained data.

## 6 Conclusion

This paper analyzes mortality in the 1918 influenza pandemic in the Kingdom of Württemberg and the effect of income and pollution on pandemic severity. The “Spanish Flu” reached the southwest German state during the hardships of the First World War. The suffering due to starvation and the war, causing more than 72,000 deaths military personnel in Württemberg, in combination with a (self-)censored press could explain that the pandemic received little public attention and did not leave a lasting impression in the collective memory of the population. To put this in perspective, the 72,000 deaths military personnel account for about 30 deaths per 1,000 inhabitants in 1910, whereas the estimates of the pandemic mortality rate in Württemberg presented in the paper range between 2.3 and 4.1 excess deaths per 1,000 persons (see Section 2).

However, the 1918 influenza pandemic led to a significant increase in all-cause mortality rates in Württemberg of 23 percent relative to 1917. The paper shows that this increase was larger in poor and highly polluted parishes. Parishes with high levels of coal-fired power plant capacity

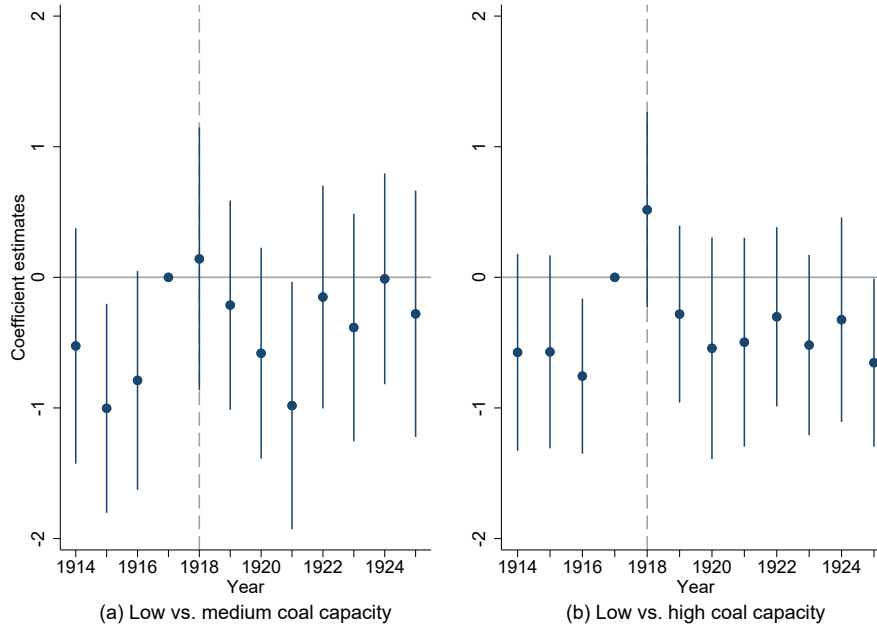


**Figure 10:** Estimated difference in mortality rate changes at the county level by coal capacity

*Notes:* The graph depicts differences in mortality rates between counties in the middle and low coal capacity tercile (left panel) and the high and low coal capacity tercile (right panel), as estimated in an event study regression. Differences are expressed relative to the baseline difference in 1917. Point estimates are marked by a dot. The vertical bands indicate the 95 percent confidence interval of each estimate. The red dashed vertical line indicates the pandemic year 1918. Author’s design.

within 50 kilometers faced an additional increase of 1.0 death per 1,000 population relative to medium and low polluted parishes. Moreover, the relative increase in mortality rates was lower in medium and high-income parishes by 1.4 and 1.0 deaths per 1,000 population, relative to low-income parishes. These results are robust to changes in model specifications, variable definitions, and the sample. However, the focus on coal-fired power plant capacity might render the pollution effects at the lower bound because it is an imperfect measure of the actual local pollution levels.

The data show that the mortality burden of the 1918 influenza pandemic was lower in Württemberg compared to other German states, even though Württemberg was relatively poor by German standards. The newly calculated estimates for the German excess mortality rate are between 5.4 and 5.9 excess deaths per 1,000 population. One reason might be the relative backwardness of Württemberg’s economy, resulting in low usage of coal compared to other German states and foreign countries. For instance, in the sample of US cities in Clay et al. (2018), the average installed coal-fired capacity within 30 miles (48.3 kilometers) is 182.8 MW, while it is only 24.9 MW (within 50 kilometers) in Württemberg. In Clay et al. (2018), medium coal capacity cities have on average an installed capacity of 50.7 MW, while in Württemberg, only parishes in the highest tercile reach this level. In line with this argument, the effect for medium coal capacity parishes is insignificant in Württemberg, whereas Clay et al. (2018) find an effect also for medium coal capacity cities. Thus, the lack of coal that contributed to Württemberg’s

economic backwardness might have been beneficial in reducing the pandemic’s death toll.

Furthermore, Württemberg had a relatively high share of agricultural employment at the beginning of WWI. Possibly, this made the Kingdom more resistant to the Allied blockade and resulting food shortages.

## References

- Acemoglu, D., Cantoni, D., Johnson, S., and Robinson, J. A. (2011). The consequences of radical reform: The French Revolution. *American Economic Review*, 101(7):3286–3307.
- Acuna-Soto, R., Viboud, C., and Chowell, G. (2011). Influenza and pneumonia mortality in 66 large cities in the United States in years surrounding the 1918 pandemic. *PLoS ONE*, 6(8):e23467.
- Ansart, S., Pelat, C., Boelle, P.-Y., Carrat, F., Flahault, A., and Valleron, A.-J. (2009). Mortality burden of the 1918-1919 influenza pandemic in Europe. *Influenza and Other Respiratory Viruses*, 3(3):99–106.
- Bailey, R. E., Hatton, T. J., and Inwood, K. (2018). Atmospheric pollution, health, and height in late nineteenth century Britain. *The Journal of Economic History*, 78(4):1210–1247.
- Barro, R., Ursúa, J., and Weng, J. (2020). The coronavirus and the great influenza pandemic: Lessons from the “Spanish Flu” for the coronavirus’s potential effects on mortality and economic activity. NBER Working Paper 26866.
- Basco, S., Domenech, J., and Rosés, J. R. (2021). Unequal Mortality during the Spanish Flu. CEPR Discussion Papers 15783, C.E.P.R. Discussion Papers.
- Bauernschuster, S., Driva, A., and Hornung, E. (2020). Bismarck’s health insurance and the mortality decline. *Journal of the European Economic Association*, 18(5):2561–2607.
- Beach, B., Clay, K., and Saavedra, M. H. (2020). The 1918 influenza pandemic and its lessons for COVID-19. NBER Working Paper 27673.
- Beach, B. and Hanlon, W. W. (2017). Coal smoke and mortality in an early industrial economy. *The Economic Journal*, 128(615):2652–2675.
- Bengtsson, T., Dribe, M., and Eriksson, B. (2018). Social class and excess mortality in Sweden during the 1918 influenza pandemic. *American Journal of Epidemiology*, 187(12):2568–2576.
- Bloom-Feshbach, K., Simonsen, L., Viboud, C., Mølbak, K., Miller, M. A., Gottfredsson, M., and Andreassen, V. (2011). Natality decline and miscarriages associated with the 1918 influenza pandemic: The Scandinavian and United States experiences. *The Journal of Infectious Diseases*, 204(8):1157–1164.
- Blum, M. (2011). Government decisions before and during the First World War and the living standards in Germany during a drastic natural experiment. *Explorations in Economic History*, 48(4):556–567.
- Blum, M. (2013). War, food rationing, and socioeconomic inequality in Germany during the First World War. *The Economic History Review*, 66(4):1063–1083.
- Bogusat, H. (1923). Die Influenza-Epidemie 1918–19 im Deutschen Reiche. *Arbeiten aus dem Reichsgesundheitsamt*, 53:443–466.
- Bootsma, M. C. J. and Ferguson, N. M. (2007). The effect of public health measures on the 1918 influenza pandemic in U.S. cities. *Proceedings of the National Academy of Sciences*, 104(18):7588–7593.
- Brainerd, E. and Siegler, M. V. (2003). The economic effects of the 1918 influenza epidemic. Technical Report 3791, CEPR Working Paper.
- Braun, S. T. and Franke, R. (2019). Railways, growth, and industrialisation in a developing German economy, 1829-1910. MPRA Paper 93644, University Library of Munich, Germany.

- Carillo, M. F. and Jappelli, T. (2020). Pandemics and local economic growth: Evidence from the great influenza in Italy. Technical Report 568, CSEF Working Paper.
- Chay, K. Y. and Greenstone, M. (2003). The impact of air pollution on infant mortality: Evidence from geographic variation in pollution shocks induced by a recession. *The Quarterly Journal of Economics*, 118(3):1121–1167.
- Chowell, G., Bettencourt, L. M. A., Johnson, N., Alonso, W. J., and Viboud, C. (2007). The 1918–1919 influenza pandemic in England and Wales: spatial patterns in transmissibility and mortality impact. *Proceedings of the Royal Society B: Biological Sciences*, 275(1634):501–509.
- Cilek, L., Chowell, G., and Fariñas, D. R. (2018). Age-specific excess mortality patterns during the 1918–1920 influenza pandemic in Madrid, Spain. *American Journal of Epidemiology*, 187(12):2511–2523.
- Clay, K., Lewis, J., and Severnini, E. (2018). Pollution, infectious disease, and mortality: Evidence from the 1918 Spanish Influenza Pandemic. *The Journal of Economic History*, 78(4):1179–1209.
- Clay, K., Lewis, J., and Severnini, E. (2019). What explains cross-city variation in mortality during the 1918 influenza pandemic? Evidence from 438 U.S. cities. *Economics & Human Biology*, 35:42–50.
- Cox, M. E. (2015). Hunger games: Or how the allied blockade in the First World War deprived German children of nutrition, and Allied food aid subsequently saved them. *The Economic History Review*, 68(2):600–631.
- Currie, J. and Neidell, M. (2005). Air pollution and infant health: What can we learn from California's recent experience? *The Quarterly Journal of Economics*, 120(3):1003–1030.
- Dahl, C. M., Hansen, C. W., and Jensen, P. S. (2020). The 1918 epidemic and a v-shaped recession: Evidence from municipal income data.
- Deaton, A. (2003). Health, inequality, and economic development. *Journal of Economic Literature*, 41(1):113–158.
- Dettmar, G. (1913). *Statistik der Elektrizitätswerke in Deutschland nach dem Stand vom 1. April 1913*. Julius Springer, Berlin.
- Erkoreka, A. (2020). Safe villages during the 1918–1919 influenza pandemic in Spain and Portugal. *Journal of Preventive Medicine and Hygiene*, 61(2):137–142.
- Fernihough, A. and O'Rourke, K. H. (2020). Coal and the european industrial revolution. *The Economic Journal*.
- Flik, R. (2001). Von der Agrar- zur Dienstleistungsgesellschaft: Baden-Württemberg 1800–2000. In Cost, H. and Körber-Weik, M., editors, *Die Wirtschaft von Baden-Württemberg im Umbruch*, pages 44–68. Kohlhammer, Stuttgart.
- Fotheringham, A. S. and Wong, D. W. (1991). The modifiable areal unit problem in multivariate statistical analysis. *Environment and planning A*, 23(7):1025–1044.
- Frank, H. (1993). *Regionale Entwicklungsdisparitäten im deutschen Industrialisierungsprozeß 1849- 1939, Eine empirisch-analytische Untersuchung*. PhD thesis, Westfälische Wilhelms-Universität Münster.
- Gallardo-Albarrán, D. (2020). Sanitary infrastructures and the decline of mortality in Germany, 1877–1913. *The Economic History Review*, 73(3):730–757.
- Gotway, C. A. and Young, L. J. (2002). Combining incompatible spatial data. *Journal of the American Statistical Association*, 97(458):632–648.
- Grantz, K. H., Rane, M. S., Salje, H., Glass, G. E., Schachterle, S. E., and Cummings, D. A. T. (2016). Disparities in influenza mortality and transmission related to sociodemographic factors within Chicago in the pandemic of 1918. *Proceedings of the National Academy of Sciences*, 113(48):13839–13844.
- Grebler, L. and Winkler, W. (1940). *The Cost of the World War to Germany and to Austria-Hungary*. Yale University Press, New Haven.

- Herwig, H. (2014). *The First World War: Germany and Austria-Hungary 1914–1918*. Bloomsbury, London, England; New York, New York.
- Herzig, T., Fehrenbach, P., and Drummer, M. (2017). Statistik der öffentlichen Elektrizitätsversorgung Deutschlands 1890 bis 1913.
- Hogbin, V. (1985). Railways, disease and health in South Africa. *Social Science & Medicine*, 20(9):933–938.
- Hornbeck, R. (2012). The enduring impact of the american dust bowl: Short- and long-run adjustments to environmental catastrophe. *American Economic Review*, 102(4):1477–1507.
- Howard, N. P. (1993). The social and political consequences of the allied food blockade of Germany, 1918–19. *German History*, 11(2):161–188.
- Jaspers, I., Ciencewicky, J. M., Zhang, W., Brighton, L. E., Carson, J. L., Beck, M. A., and Madden, M. C. (2005). Diesel exhaust enhances influenza virus infections in respiratory epithelial cells. *Toxicological Sciences*, 85(2):990–1002.
- Johnson, N. P. A. S. (2001). *Aspects of the historical geography of the 1918–19 influenza pandemic in Britain*. PhD thesis, University of Cambridge.
- Johnson, N. P. A. S. and Mueller, J. (2002). Updating the accounts: Global mortality of the 1918–1920 “Spanish” influenza pandemic. *Bulletin of the History of Medicine*, 76(1):105–115.
- Kaiserliches Statistisches Amt (1915). Die Bevölkerung im Deutschen Reiche am 1. Dezember 1910. *Statistik des Deutschen Reichs*, 240.
- Karlsson, M., Nilsson, T., and Pichler, S. (2014). The impact of the 1918 Spanish flu epidemic on economic performance in Sweden. *Journal of Health Economics*, 36:1–19.
- Kommission für geschichtliche Landeskunde in Baden-Württemberg and Landesvermessungsamt Baden-Württemberg (1972). Historischer Atlas von Baden-Württemberg. Karte 2,2: Gemeindegrenzenkarte.
- Königliches Statistisches Landesamt (1900). *Die Standorte der Gewerbe Württembergs nach Gemeinden am 14. Juni 1895: Gewerbetopographie*. W. Kohlhammer Verlag, Stuttgart.
- Königliches Statistisches Landesamt (1905). *Württembergische Jahrbücher für Statistik und Landeskunde 1904*. W. Kohlhammer, Stuttgart.
- Königliches Statistisches Landesamt (1910). *Württembergische Gemeindestatistik. Zweite Ausgabe nach dem Stand vom Jahr 1907*. W. Kohlhammer Verlag, Stuttgart.
- Königliches Statistisches Landesamt (1911). *Königlich-Württembergisches Hof- und Staats-Handbuch*. W. Kohlhammer Verlag, Stuttgart.
- Kunz, A. and Zipf, A. (2008). HGIS Germany: Historical information system of the German states, 1820 to 1914. Technical report, Leibniz-Institut für Europäische Geschichte and i3mainz - Institut für Raumbezogene Informations- und Messtechnik.
- Levy, J. I., Spengler, J. D., Hlinka, D., Sullivan, D., and Moon, D. (2002). Using CALPUFF to evaluate the impacts of power plant emissions in Illinois: model sensitivity and implications. *Atmospheric Environment*, 36(6):1063–1075.
- Losch, H. J. (1912). Die Veränderungen im wirtschaftlichen und gesellschaftlichen Aufbau der Bevölkerung Württembergs nach den Ergebnissen der Berufs- und Betriebszählung vom 12. Juni 1907. In *Württembergische Jahrbücher für Statistik und Landeskunde*, volume 1911, pages 94–190. W. Kohlhammer Verlag, Stuttgart.
- Mamelund, S.-E. (2006). A socially neutral disease? Individual social class, household wealth and mortality from Spanish influenza in two socially contrasting parishes in Kristiania 1918–19. *Social Science & Medicine*, 62(4):923–940.

- Mamelund, S.-E. (2018). 1918 pandemic morbidity: The first wave hits the poor, the second wave hits the rich. *Influenza and Other Respiratory Viruses*, 12(3):307–313.
- Marquardt, E. (1985). *Geschichte Württembergs*. Deutsche Verlags-Anstalt, Stuttgart.
- Max Planck Institute for Demographic Research (MPIDR) and Chair for Geodesy and Geoinformatics, University of Rostock (CGG) (2011). MPIDR Population History GIS Collection (partly based on Bundesamt für Kartographie und Geodäsie). Mosaic Project.
- Michels, E. (2010). Die Spanische Grippe 1918/19. Verlauf, Folgen und Deutungen in Deutschland im Kontext des Ersten Weltkriegs. *Vierteljahrshefte für Zeitgeschichte*, 58(1):1–33.
- Mills, C. E., Robins, J. M., and Lipsitch, M. (2004). Transmissibility of 1918 pandemic influenza. *Nature*, 432(7019):904–906.
- Murray, C. J. L., Lopez, A. D., Chin, B., Feehan, D., and Hill, K. H. (2006). Estimation of potential global pandemic influenza mortality on the basis of vital registry data from the 1918–20 pandemic: A quantitative analysis. *The Lancet*, 368(9554):2211–2218.
- Ogilvie, S. (2004). Guilds, efficiency, and social capital: Evidence from German proto-industry. *The Economic History Review*, 57(2):286–333.
- Ogilvie, S. (2019). *The European Guilds*. Princeton University Press, Princeton, NJ.
- Ott, H., Herzig, T., Allgeier, R., and Fehrenbach, P. (1981). *Elektrizitätsversorgung von Baden, Württemberg und Hohenzollern 1913/14*, chapter 11, 9. Historischer Atlas Baden-Württemberg.
- Ott, W.-R. (1971). *Grundlageninvestitionen in Württemberg. Maßnahmen zur Verbesserung der materiellen Infrastruktur in der Zeit vom Beginn des 19. Jahrhunderts bis zum Ende des Ersten Weltkrieges*. phdthesis, Ruprecht-Karl-Universität Heidelberg, Heidelberg.
- Patterson, K. D. and Pyle, G. F. (1991). The geography and mortality of the 1918 influenza pandemic. *Bulletin of the History of Medicine*, 65(1):4–21.
- Pitz, M., Cyrus, J., Karg, E., Wiedensohler, A., Wichmann, H.-E., and Heinrich, J. (2003). Variability of apparent particle density of an urban aerosol. *Environmental Science & Technology*, 37(19):4336–4342.
- Reid, A. (2005). The effects of the 1918–1919 influenza pandemic on infant and child health in Derbyshire. *Medical History*, 49(1):29–54.
- Rothenbacher, F. (2002). *The European Population 1850–1945*. Palgrave, Basingstoke.
- Statistisches Landesamt (1922). *Württembergische Jahrbücher für Statistik und Landeskunde 1919/20*. W. Kohlhammer, Stuttgart.
- Statistisches Landesamt (1923). *Statistisches Handbuch für Württemberg 1914/21*. W. Kohlhammer, Stuttgart.
- Statistisches Landesamt (1928). *Statistisches Handbuch für Württemberg 1922/26*. W. Kohlhammer, Stuttgart.
- Statistisches Landesamt Baden-Württemberg (2008). *Volkszählungen in Württemberg 1834 bis 1925*.
- Statistisches Reichsamt (1920). *Statistisches Jahrbuch für das Deutsche Reich 1919*. Puttkammer & Mühlbrecht, Berlin.
- Statistisches Reichsamt (1921a). *Statistisches Jahrbuch für das Deutsche Reich 1920*. Puttkammer & Mühlbrecht, Berlin.
- Statistisches Reichsamt (1921b). *Wirtschaft und Statistik*, volume 1. Reimar Hobbing, Berlin.
- Statistisches Reichsamt (1922). *Statistisches Jahrbuch für das Deutsche Reich 1921/22*. Verlag für Politik und Wirtschaft, Berlin.

- Statistisches Reichsamt (1924). *Statistisches Jahrbuch für das Deutsche Reich 1923*. Verlag für Politik und Wirtschaft, Berlin.
- Statistisches Reichsamt (1925). *Statistisches Jahrbuch für das Deutsche Reich 1924/1925*. Verlag für Politik und Wirtschaft, Berlin.
- Stein, A. F., Draxler, R. R., Rolph, G. D., Stunder, B. J. B., Cohen, M. D., and Ngan, F. (2015). NOAA's HYSPLIT atmospheric transport and dispersion modeling system. *Bulletin of the American Meteorological Society*, 96(12):2059–2077.
- Steinthal, E. (1918). Beobachtungen an “Spanischer Krankheit”. *Medicinisches Correspondenz-Blatt des Württembergischen ärztlichen Landesvereins*, 88(42):367–368.
- Sydenstricker, E. (1931). The incidence of influenza among persons of different economic status during the epidemic of 1918. *Public Health Reports (1896-1970)*, 46(4):154.
- Taubenberger, J. K., Kash, J. C., and Morens, D. M. (2019). The 1918 influenza pandemic: 100 years of questions answered and unanswered. *Science Translational Medicine*, 11(502):eaau5485.
- von Moser, O. (1927). *Die Württemberger im Weltkrieg*. Chr. Belser AG, Stuttgart.
- Weil, D. N. (2014). Health and economic growth. In *Handbook of Economic Growth*, pages 623–682. Elsevier.
- Witte, W. (2003). The plague that was not allowed to happen: German medicine and the influenza epidemic of 1918–19 in Baden. In Phillips, H. and Killingray, D., editors, *The Spanish Influenza Pandemic of 1918–19*, pages 49–57. Routledge, New York.
- Wong, C. M., Yang, L., Thach, T. Q., Chau, P. Y. K., Chan, K. P., Thomas, G. N., Lam, T. H., Wong, T. W., Hedley, A. J., and Peiris, J. M. (2009). Modification by influenza on health effects of air pollution in Hong Kong. *Environmental Health Perspectives*, 117(2):248–253.
- Wu, X., Nethery, R. C., Sabath, M. B., Braun, D., and Dominici, F. (2020). Air pollution and COVID-19 mortality in the united states: Strengths and limitations of an ecological regression analysis. *Science Advances*, 6(45):eabd4049.

## A Appendix

### A.1 Württemberg in the German Empire

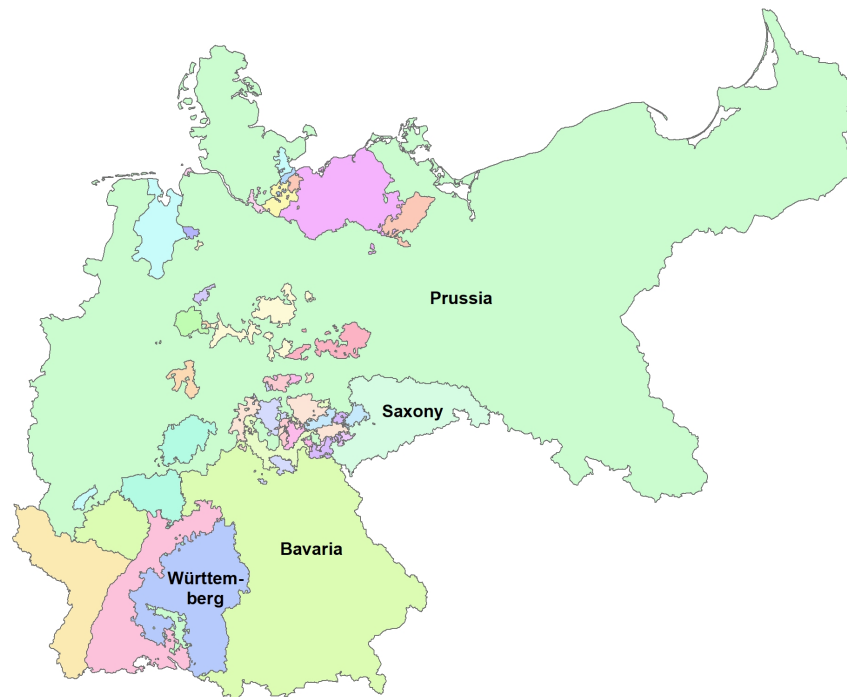


Figure A-1: The German Empire in 1871

*Notes:* The figure shows the German Empire in its 1871 borders. Labels mark the four Kingdoms that were part of the German Empire (namely, the Kingdoms of Bavaria, Prussia, Saxony and Württemberg).

*Source:* Max Planck Institute for Demographic Research (MPIDR) and Chair for Geodesy and Geoinformatics, University of Rostock (CGG) (2011). Author's design.

### A.2 Energy supply during WWI

If the First World War caused energy production and coal usage to drop dramatically, it could bias the pollution effect estimates because the measure is based on installed capacity. However, already before WWI electric energy was widely used in manufacturing industries. Hence, it was important for the war efforts of the German Empire to secure electric energy supply.

In Section 2.1, the paper refers to coal usage statistics for Württemberg. It is shown that in 1918 the average annual coal consumption per capita was 1,013 kilograms and in 1913 it was 1,000 kilograms per capita (Statistisches Landesamt, 1923). Thus, there is no significant change in coal usage in Württemberg. The same holds for the German Empire. In 1913 the annual average coal usage per capita was 3,870 kilograms of coal, while in 1917 it was 3,732 kilograms

(Statistisches Reichsamt, 1925).

Often, the total output of coal in the German Empire is used to illustrate a decline in energy supply during WWI. Table A-1 shows the total coal output of the German Empire from 1913 to 1920. The total black coal output decreases from 190,109 thousand tons in 1913 to 158,254 thousand tons in 1918 (Statistisches Reichsamt, 1921b). This decline seemingly contradicts the previous point of a relatively stable coal consumption per capita during WWI. However, the total output does not account for boundary changes of the German Empire. Moreover, the decline in black coal output could be largely offset by other measures. The output of lignite increased in this period from 87,233 to 100,599 thousand tons. In addition, black coal exports halved from 34,598 thousand tons in 1913 to 15,230 thousand tons in 1917 and also lignite exports were reduced (Statistisches Reichsamt, 1925). These measures could also offset the decline in coal imports due to the sea blockade.

**Table A-1:** Coal output 1913–1920 in thousand tons

Year	Black coal				Lignite
	Empire	Ruhr area	Upper Silesia	Saar Basin	Empire
1913	190,109	114,487	43,435	13,217	87,233
1914	161,385	98,285	36,996	10,032	83,694
1915	146,868	86,778	38,107	8,384	87,694
1916	159,170	94,563	41,723	8,903	94,180
1917	167,747	99,365	42,752	10,265	95,543
1918	158,254 <sup>†</sup>	96,016	39,648	9,989	100,599
1919	116,681 <sup>†</sup>	67,926	25,697	8,990	93,843
1920	140,757 <sup>†</sup>	84,986	31,686	9,410	111,634

*Notes:* The table shows coal output in the German Empire between 1913 and 1920 in thousand metric tons. <sup>†</sup> Excluding Lorraine. *Source:* Statistisches Reichsamt (1921b).

Another measure to illustrate energy consumption is the actual energy production of power plants in Württemberg. In 1917 the 31 largest power plants in Württemberg, accounting for five-sixths of the total amount of generated power, produced 176,515.4 MWh of energy and reached an average capacity factor of 25.2 percent (Ott, 1971; Statistisches Landesamt, 1923, 1928).<sup>38</sup> Thus, the utilization of installed power during WWI was even higher than in 1926 when the largest power plants in Württemberg had a capacity factor of 23.0 percent (Statistisches

<sup>38</sup>The capacity factor is the ratio of energy output over one year to the maximum possible energy output (installed capacity times 365 days times 24 hours). The energy production includes also hydroelectric power plants and therefore might overestimate the capacity factor of coal-fired power plants in 1917. However, the power plants in Ellwangen and Heilbronn, for instance, had a capacity factor of 20.8 and 23.9 percent in 1917, while 99 and 100 percent of the installed capacity was based on steam engines, respectively. Moreover, the purely hydroelectric power plant in Ludwigsburg achieved a comparable capacity factor of 26.3 percent in 1917 (Statistisches Landesamt, 1923).

Landesamt, 1928).

These statistics show that the energy production was relatively stable during WWI. Therefore, it is likely that also pollution from coal-fired power plants was largely unaffected by the war.

### A.3 Excess mortality estimations

In this section, I present the definitions and calculations of the excess mortality statistics presented in Section 2.3.

Similar to Ansart et al. (2009), I use the monthly all-cause mortality statistics for Württemberg (Statistisches Landesamt, 1922). However, their data set covers the period 1906–1922 for Germany, while my data only cover the years 1914–1919. Yet, the shorter time period might be advantageous because it could prevent the downward bias in baseline mortality rates due to the inclusion of pre-war years.<sup>39</sup> For the calculations I normalize monthly all-cause deaths by population (annually average population from Statistisches Landesamt (1928)) to get monthly mortality rates by 1,000 population. The monthly baseline mortality rate  $B_t$  is based on a linear model

$$B_t = \alpha_0 + \alpha_t t + \gamma_1 \cos(2\pi t/n) + \delta_1 \sin(2\pi t/n) + \gamma_2 \cos(4\pi t/n) + \delta_2 \sin(4\pi t/n) + \epsilon_t, \quad (\text{A-1})$$

with  $n = 12$  and  $t = \{1, 2, \dots, 12\}$ . The model parameters are estimated using the monthly mortality rate in 1914–1917, excluding in each August to July period the trimester with the highest mortality rates. Based on the estimated model parameters, the baseline mortality is predicted for 1918 and 1919. An excess mortality period is identified if the mortality rate is above the threshold of  $B_t + 1.96\text{sd}(\epsilon_t)$  for at least two consecutive months.

Figure A-2 shows the monthly all-cause mortality rate per 1,000 population (solid line), the estimated baseline mortality rate  $B_t$  (dashed line) and the threshold value (dotted line). The excess mortality period in 1918–1919 is identified for the months October 1918 to January 1919, highlighted by gray shading in Figure A-2. The cumulative excess mortality rate is 3.8 deaths per 1,000 population.

---

<sup>39</sup>Indeed, Ansart et al. (2009) identify the excess mortality period for Germany to start in March 1918. This could be due to an under estimation of baseline mortality rates during the First World War. Thus, if we assume that the excess mortality in March 1918 was not caused by the influenza virus, the cumulative excess mortality rate attributed to the influenza pandemic is likely upward biased.

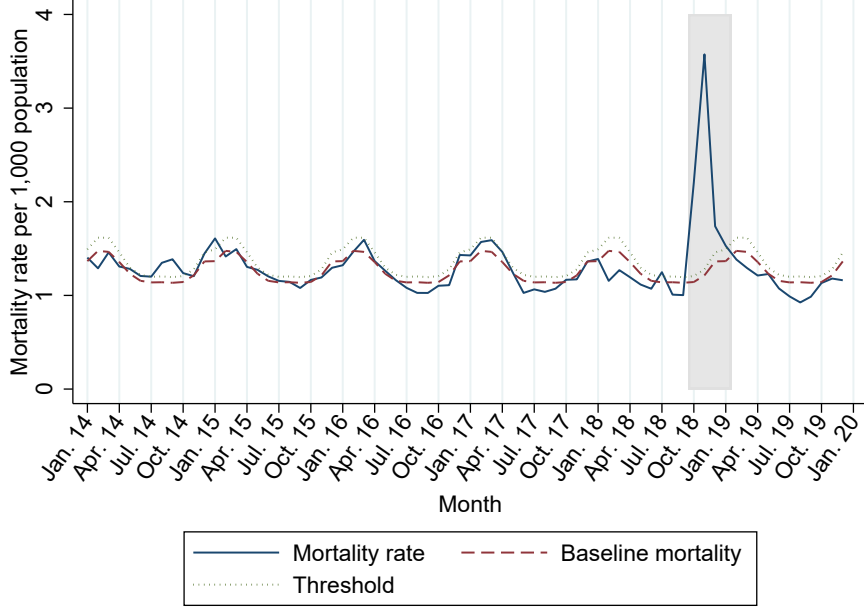


**Figure A-2:** Monthly excess mortality

*Notes:* The graph depicts monthly all-cause mortality rate in the Kingdom of Württemberg (solid line), the monthly baseline mortality rate  $B_t$  (dashed line), and the threshold,  $B_t + 1.96 \cdot \text{sd}(\epsilon_t)$  (dotted line) for the years 1914 to 1919. The mortality rate does not account for the number of death of military personnel and stillbirths. *Source:* Statistisches Landesamt (1922). Author’s design.

Murray et al. (2006) calculate the excess mortality during the “Spanish Flu” as the sum over the deviations in mortality in 1918–1920 from the average in 1915–1917 and 1921–1923. Formally, the excess mortality  $EM$  is

$$EM_{1918-20} = \sum_{1918}^{1920} \left( M_t - \frac{M_{1915} + M_{1916} + M_{1917} + M_{1921} + M_{1922} + M_{1923}}{6} \right), \quad (\text{A-2})$$

with  $M_t$  defined as the all-cause mortality in year  $t$ . To calculate the excess mortality rate, the resulting value of  $EM_{1918-20}$  is divided by 1,000 population. Thus, the excess mortality rate for Württemberg is 2.3 (Statistisches Landesamt, 1928).

Barro et al. (2020) apply the method from Murray et al. (2006), but use all influenza-related deaths if available. For the calculation I include all deaths from influenza (*Influenza*), pneumonia (*Lungenentzündung*), other diseases of the respiratory organs (*Krankheiten der Atmungsorgane*), tuberculosis (*Tuberkulose der Lungen (Lungenschwindsucht)*), and whooping cough (*Keuchhusten*). A similar list of diseases is underlying the excess mortality calculations for England and Wales in Johnson and Mueller (2002). The cause-specific mortality data for 1915–1923 are from archival material (Staatsarchiv Ludwigsburg E 258 VII Bü 662). The excess mortality rate per 1,000 population for the years 1918–1920 is 3.9.

Table A-2 shows excess mortality rate estimates for Germany, its states, and Prussian provinces. I digitized the case-specific mortality and population data from various volumes of the *Statistisches Jahrbuch für das Deutsche Reich* (Statistisches Reichsamt, 1920, 1921a, 1922, 1924, 1925). The calculations generally follow the approach of Murray et al. (2006) for all-cause mortality (Columns (1) and (2)) and influenza-related mortality (Columns (3) and (4)). However, in Columns (2) and (4) the excess mortality rate is defined as the aggregate deviation from the average in 1921–23 because for 1915–17 the sources do not report mortality statistics for Prussian provinces.

Moreover, I calculate the aggregate deviation of the mortality rates in 1918-20 from the average mortality rate in non-pandemic years, while Murray et al. (2006) use the number of deaths. This alternative specifications allows to take changes in the total number of deceased due to boundary changes into account. After WWI, Germany lost considerable parts of its territory. The boundary changes affected especially the Prussian provinces of Silesia and Posen-West Prussia. In addition, I correct total population for boundary changes within Germany, namely the transition of Pymont from Waldeck to Hanover in 1921, and the incorporation of municipalities from Brandenburg into Berlin in 1920. Neglecting these boundary changes would severely bias the excess mortality rate estimates upwards in case of territorial losses.

The estimated excess mortality rates for Germany are 5.4 in Column (1) and 5.9 in Column (3) using all-cause mortality and influenza-related mortality respectively. Thus, the estimates for Germany provide further evidence that the true excess mortality rate of the influenza pandemic is within the range of 3.8 to 7.8, which is the range of previous estimates. For Württemberg the respective estimates are slightly higher than above with 2.5 and 4.0 excess deaths per 1,000 population. The difference is due to slightly higher mortality statistics for the years 1919 and 1920 reported in Statistisches Reichsamt (1924). Nevertheless, Table A-2 shows that Wüttemberg had one of the lowest excess mortality rates in Germany.

The excess mortality rates in Columns (2) and (4) are on average higher than in Columns (1) and (3) but highly correlated. The on average higher excess mortality is driven by the exclusion of the higher average mortality rates observed during WWI. Thus, these estimates are not directly comparable to previous results.

It is beyond the scope of this paper to evaluate the various excess mortality rate estimates for Germany and its regions. However, the estimates presented here might inform future research

on the mortality burden during the 1918–1919 influenza pandemic in Germany.

**Table A-2:** Excess mortality rates in Germany

Region	Excess mortality rate 1918–20, deviation from:			
	1915–17		1915–17	
	1921–23	1921–23	1921–23	1921–23
	All-cause		Influenza related	
	(1)	(2)	(3)	(4)
Germany	5.4	6.1	5.9	6.0
Prussia	6.6	7.8	6.8	7.0
<i>East Prussia</i>		6.0		5.1
<i>Berlin</i>		6.7		6.2
<i>Brandenburg</i>		4.1		5.2
<i>Pomerania</i>		6.0		6.0
<i>Silesia</i>		6.2		8.1
<i>Saxony</i>		6.6		6.3
<i>Schleswig-Holstein</i>		5.5		4.4
<i>Hanover</i>		6.7		5.8
<i>Westphalia</i>		8.1		8.3
<i>Hesse-Nassau</i>		8.8		7.2
<i>Rhineland</i>		10.1		8.1
<i>Hohenzollern</i>		3.5		3.8
<i>Posen-West Prussia</i>		8.2		6.0
Bavaria	3.1	3.8	4.2	4.8
Württemberg	2.5	3.7	4.0	4.3
Saxony	4.2	6.1	4.7	5.1
Baden	4.2	5.2	4.8	5.4
Hesse	5.3	7.0	5.2	5.9
Thuringia	7.1	8.2	5.7	5.8
Oldenburg	5.6	6.9	6.2	6.6
Brunswick	8.0	9.4	7.0	7.8
Anhalt	7.0	7.9	6.5	6.6
Lippe	4.0	6.1	5.9	6.6
Waldeck	5.8	5.8	7.3	7.3
Schaumburg-Lippe	4.1	3.6	5.4	6.0
Hamburg	4.3	4.4	5.0	4.8
Bremen	7.6	8.1	7.0	7.3
Lübeck	2.6	3.4	4.6	5.2

*Notes:* The table shows excess mortality rate estimates for Germany and its states. Columns (1) and (2) report all-cause excess mortality rates per 1,000 population. Columns (3) and (4) report influenza related excess mortality rates per 1,000 population, including all deaths from influenza (*Influenza*), pneumonia (*Lungenentzündung*), other diseases of the respiratory organs (*Krankheiten der Atmungsorgane*), tuberculosis (*Tuberkulose der Lungen (Lungenschwindsucht)*), and whooping cough (*Keuchhusten*). Estimates in Columns (1) and (3) are based on equation (A-2). Estimates in Columns (2) and (4) are based on equation (A-2) but using only the deviation from average mortality 1921–23.

## A.4 Pollution dispersion and wind patterns

Beach and Hanlon (2017) use wind patterns to identify the causal effect of coal smoke on infant mortality in late 19th century Britain. Therefore, the authors exploit the fact that the British islands experience relatively stable southwest winds. Consequently, pollutants mainly disperse to the northeast of an emitting source. The relatively stable wind pattern allows the authors to compare mortality rates between downwind and upwind districts and find a significant effect of pollution on infant mortality.

For Württemberg, however, the climatic and topographical conditions are quite different. First, Württemberg is located in continental Europe with no coastal access, which leads to lower average wind speeds. Second, Württemberg has a hilly topography, especially compared to most parts of England. Therefore, one can observe much more turbulent wind flows. These differences affect the dispersion of pollutants in space.

Figure A-3 illustrates the dispersion of fine particulate matter (PM<sub>2.5</sub>) for an emitting location in Württemberg and Britain, namely Stuttgart and Birmingham. The figure shows twelve different sub-figures with air concentrations of fine particulate matter between 0 and 10 meters above the ground. The concentration measure is based on simulations in HYSPLIT (Stein et al., 2015). In columns (1) to (3) the emission location is Stuttgart (coordinates: 48.77, 9.18), and in column (4) it is Birmingham (52.48, -1.9). Both locations are indicated by stars in the respective figures. The dashed circle in each sub-figure shows a 50 kilometer radius around the emitting location. The dispersion model simulates the emission of 6,000 particles between 10 and 50 meters above ground over a period of 6 hours.<sup>40</sup> The simulation starts on January 1 at 6:00 am and repeats every 12 hours over the course of one year. The results of these individual simulations are combined to produce the outputs shown in Figure A-3.

Rows a), b), and c) of Figure A-3 illustrate the dispersion after one, three, and six hours. Columns (1), (2), and (4) show the annual concentration at the 95 percentile and column (3) the annual average concentration.<sup>41</sup> The different concentration levels are coded by different colors,

---

<sup>40</sup>The emission between 10 and 50 meters above ground simulates a smoke column. The simulated particles have a diameter of 2.5  $\mu\text{m}$  and a density of 1.6  $\text{g}/\text{cm}^3$  (Pitz et al., 2003). The model allows dry deposition and uses meteorological data from the NCEP/NCAR Global Reanalysis.

<sup>41</sup>The dispersion of particles is based on a probabilistic model. Thus, the illustration of percentiles excludes some trajectories that are, conditional on the meteorological data, less likely. This leads to a more compact dispersion which allows an easier interpretation of general patterns. However, this does not necessarily imply that the concentration at the 95 percentile is closer to the true spatial dispersion compared to other measures like the mean concentration in column (3).

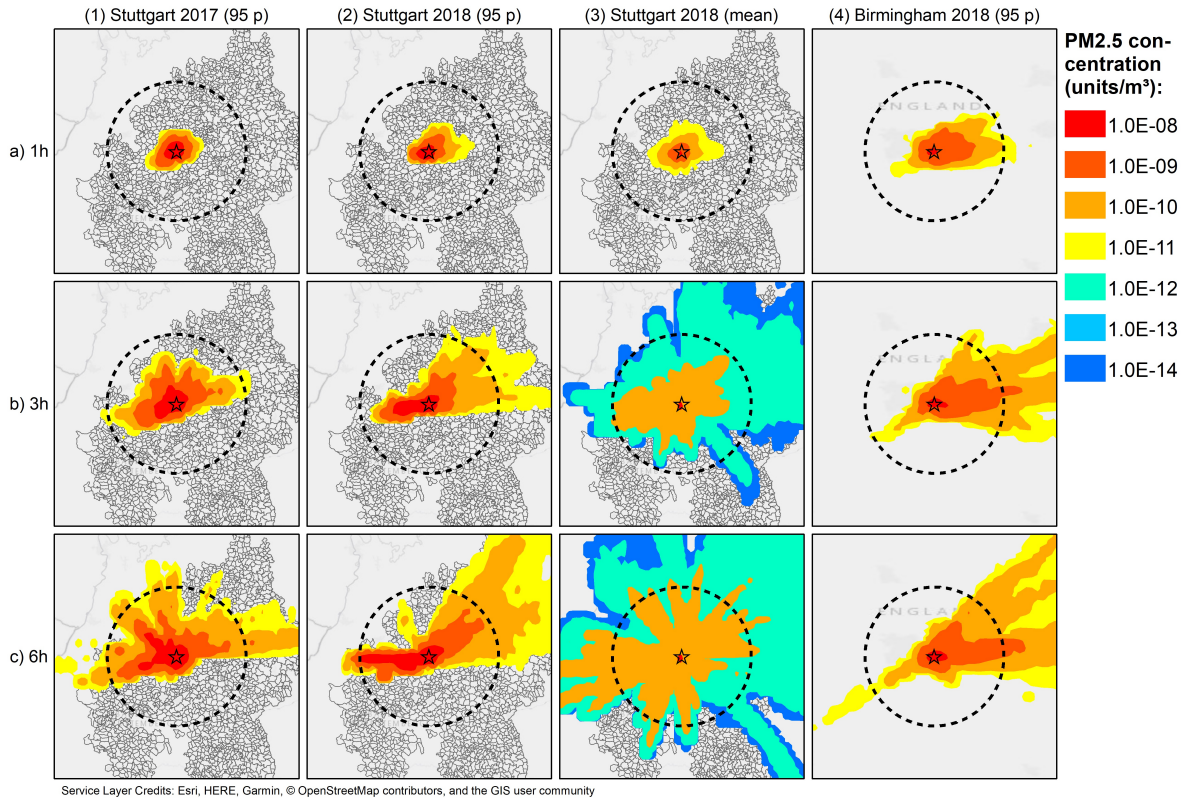


**Figure A-3:** Dispersion of fine particulate matter ( $PM_{2.5}$ )

*Notes:* The figure illustrates the dispersion of fine particulate matter ( $PM_{2.5}$ ) for an emitting location in Stuttgart (columns ((1), (2), and (3)) and Birmingham (column (4)). The sub-figures show the concentration after one (row a)), three (row b)), and six hours (row c)). Columns (1), (2), and (4), show the annual concentration at the 95 percentile and column (3) the annual average concentration. *Source:* Based on own dispersion simulations using HYSPLIT (Stein et al., 2015). Author's design.

from red (high concentration) to blue (low concentration). The actual concentration is not of importance and would also require to define a specific emission mass. However, the different color coding illustrates the decline of concentration by one order of magnitude per category.

Unfortunately, meteorological data for the simulation of dispersion in the early 20th century are not available. Therefore, the simulations are conducted for current years, specifically 2017 in column (1) and 2018 in columns (2) to (4). The results for 2017 are shown in addition to the results for 2018 to control for year specific meteorological effects. However, the simulation results for both years are quite similar.

The results in columns (1) and (2) show that after one hour, the highest concentrations at the 95 percentile are centered around the emitting location in Stuttgart (row a)). After three and six hours (rows b) and c)), however, the concentration is highest in the northern semicircle from Stuttgart. This pattern is likely driven by turbulent winds that result from the hilly topography. Moreover, the results show that the main wind direction from southwest—that is also associated

with higher average wind speeds—disperses the particles over a larger area to the northeast and thus also lowers the concentration. Hence, for the local dispersion of pollutants in Württemberg, the local turbulent winds are more important than the more frequent and stronger southwest winds.

Column (4) shows the results for the same dispersion model as in column (2) but for Birmingham. In line with the findings in Beach and Hanlon (2017), the simulations show a clear dispersion of particles to the northeast of the emitting location. However, the dispersion pattern for Birmingham differs considerably from the pattern for Stuttgart.

Finally, column (3) shows the mean concentration over one year. The results show relatively high concentration levels within 50 kilometers around Stuttgart. In combination with the more detailed analysis for modern-day coal-fired power plants in Levy et al. (2002), these simulations support the selection of a 50 kilometer radius to measure the installed coal-fired power plant capacity in this paper.

The dispersion simulations in columns (1) and (2) of Figure A-3 indicate relatively high concentration levels of fine particulate matter in the northern semicircle from the emitting location. Table A-3 shows estimation results where only the installed coal-fired capacity in the southern semicircle with 50 kilometer radius from each parish is taken into account. The increase in mortality rates between 1917 and 1918 in high coal capacity parishes relative to low coal capacity parishes is similar to the increase reported in Table 2. If anything, the effects are slightly higher. Furthermore, the point estimates in columns (2) and (3) reach higher statistical significance levels. The sign for the differential change in medium capacity parishes relative to low capacity parishes becomes positive in all four specifications and the effect is statistically significant at the 10 percent level in column (1). The results in Table A-3 might indicate a dispersion pattern to the northern semicircle. However, the results are similar to the baseline results, and the dispersion simulations in Figure A-3 column (3) also show relatively high average concentration levels within 50 kilometers. Thus, the baseline specification in this paper does not exclude power plants to the north from a given parish.

**Table A-3:** Robustness checks – Coal-fired power plants in the southern semicircle

	Mortality rate 1914–1925			
	(1)	(2)	(3)	(4)
Income medium $\times$ 1918			-1.574***	-1.245**
			(0.502)	(0.484)
Income high $\times$ 1918			-1.038**	-0.781
			(0.516)	(0.559)
Capacity medium $\times$ 1918	0.880*	0.400	0.690	0.394
	(0.510)	(0.626)	(0.526)	(0.624)
Capacity high $\times$ 1918	1.137**	1.081**	0.845*	0.921*
	(0.429)	(0.481)	(0.477)	(0.512)
Observations	21,156	21,156	21,156	21,156
FE	Yes	Yes	Yes	Yes
Year FE	Yes	Yes	Yes	Yes
Controls	No	Yes	No	Yes
Year $\times$ District FE	No	Yes	No	Yes

*Notes:* The table shows panel regression estimates of the effect of taxable income 1907 and installed coal-fired power plant capacity in the southern semicircle with 50 kilometer radius from each parish on the differential change in mortality rates. Regressions (1) and (2) show the change in medium and high coal capacity parishes between 1917 and 1918 relative to the change in low coal capacity parishes. Regressions (3) and (4) include income and coal capacity measures. All regressions include a full set of year fixed effects, parish fixed effects, and the average mortality rate 1910–1913 interacted with year fixed effects. Columns (2) and (4) include the full set of pre-treatment control variables  $X_i$  each interacted with an indicator variable for the year 1918 and year times district fixed effects. Standard errors clustered at the county level are in parentheses. \*\*\*, \*\*, and \* denote statistical significance at the 1, 5, and 10 percent level, respectively.

## A.5 Figures

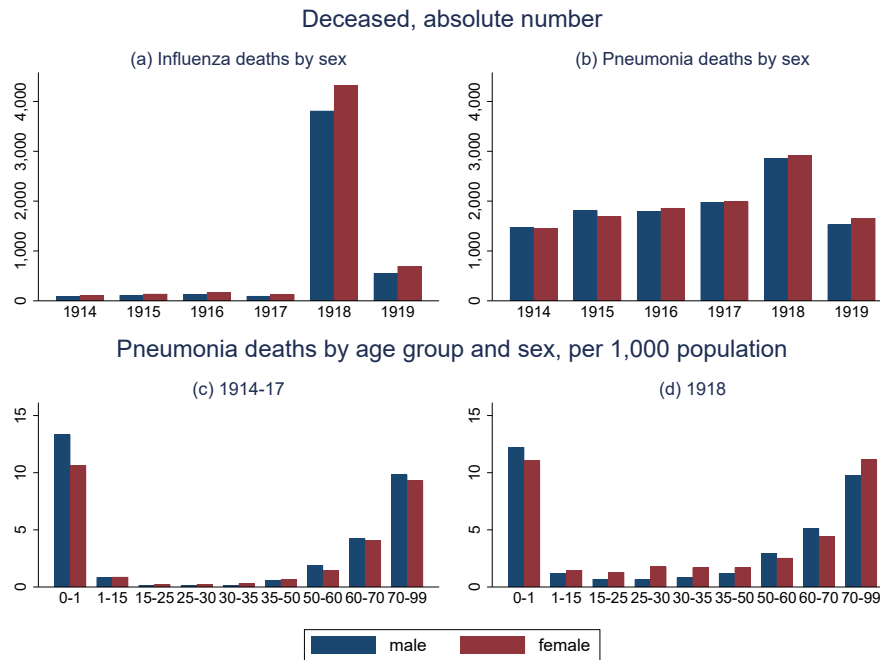


**Figure A-4:** Influenza and pneumonia mortality statistics for Württemberg

*Notes:* Figures A-4 (a) and (b) show annual influenza and pneumonia deaths by sex for the years 1914–1919, including the number of deceased among military personnel. Figure A-4 (c) depicts the annual pneumonia mortality rate by age group averaged over the years 1914–1917 and Figure A-4 (d) shows the pneumonia mortality rate by age group in 1918. *Source:* Statistisches Landesamt (1922). Author's design.

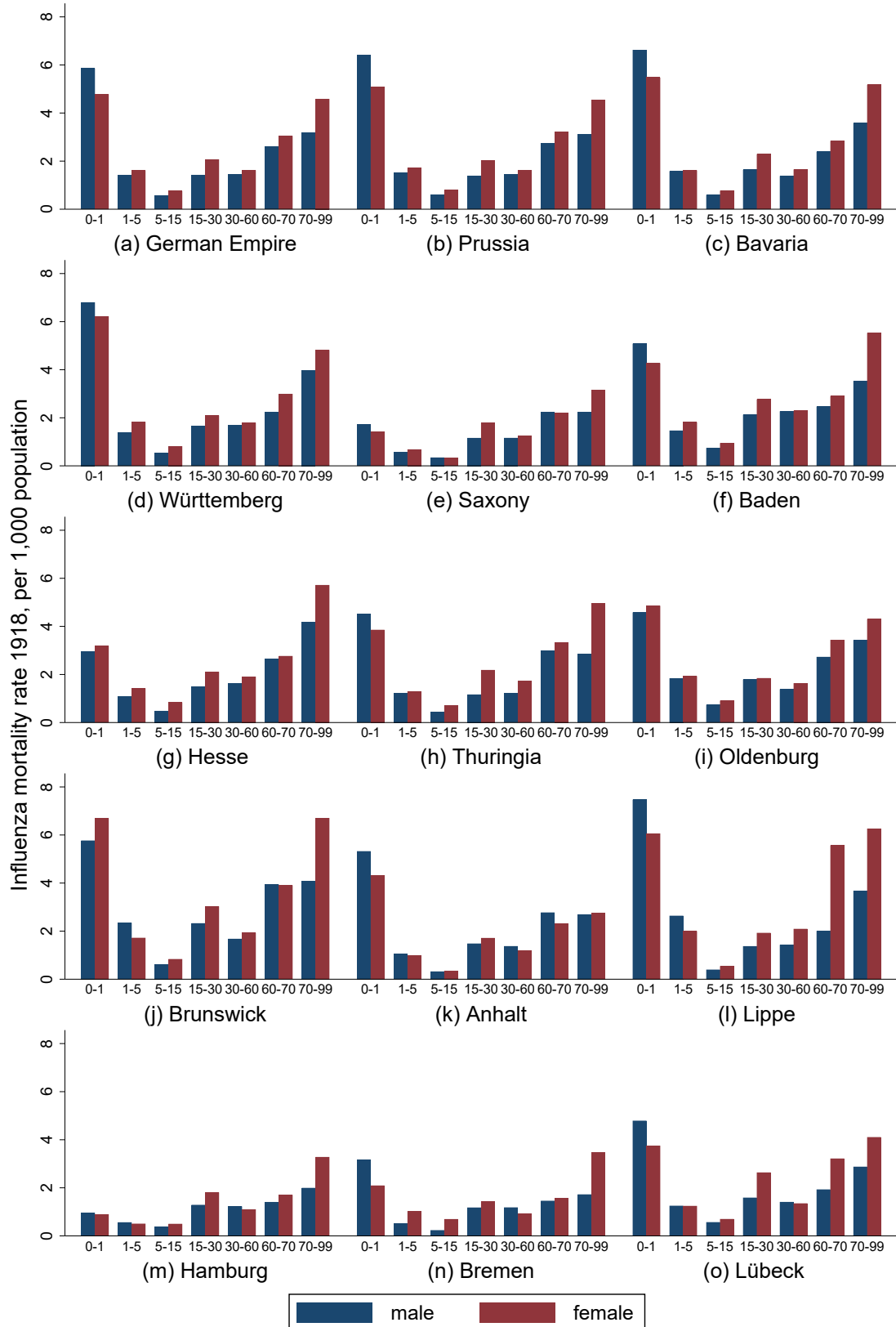


**Figure A-5:** Influenza mortality rates 1918 for the German Empire and its states, by age and sex, per 1,000 population 1910

*Notes:* Figures A-5 (a)–(o) show the influenza mortality rate by age group and sex in 1918, including the number of influenza deaths among military personnel. *Sources:* Bogusat (1923) and Kaiserliches Statistisches Amt (1915). Author's design.

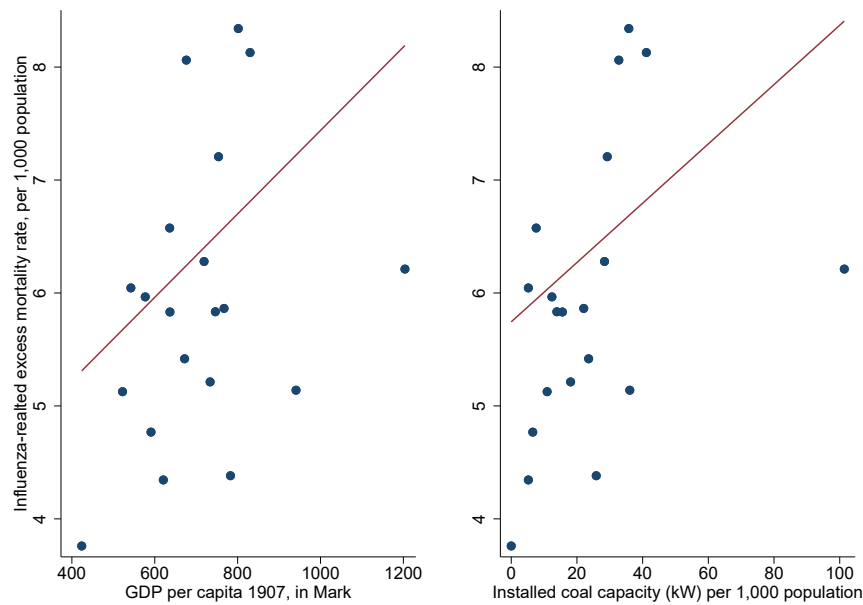


**Figure A-6:** Association of income and pollution with influenza-related excess mortality 1918–20 for German states and Prussian provinces, including Berlin

*Notes:* The graph shows the association of income (left panel) and pollution (right panel) with influenza-related excess mortality 1918–20 for German states and Prussian provinces, including Berlin. The influenza related mortality rate per 1,000 population, includes all deaths from influenza, pneumonia, other diseases of the respiratory organs, tuberculosis, and whooping cough. The excess mortality rate is the sum of deviations in 1918–20 from the average in 1921–23. The income level is measured by GDP per capita in 1907. Pollution is calculated as the installed coal-fired capacity 1913 in kW per 1,000 population. *Sources:* Herzig et al. (2017), Frank (1993), and various volumes of *Statistisches Jahrbuch für das Deutsche Reich*, see Appendix A.3 for further details. Author’s design.



**Excess mortality rate per 1,000 population 1918**

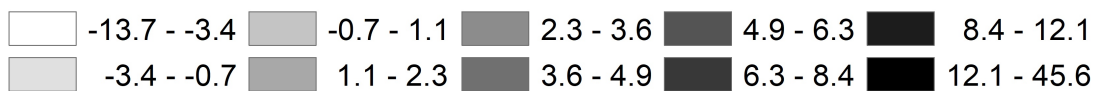


**Figure A-7:** Excess mortality rate per 1,000 population 1918

*Notes:* The map shows the excess mortality rate per 1,000 population in 1918 for all 1,763 parishes in the sample. *Sources:* Statistisches Landesamt Baden-Württemberg (2008), Staatsarchiv Ludwigsburg E 258 VII Bü 120. Author's design.

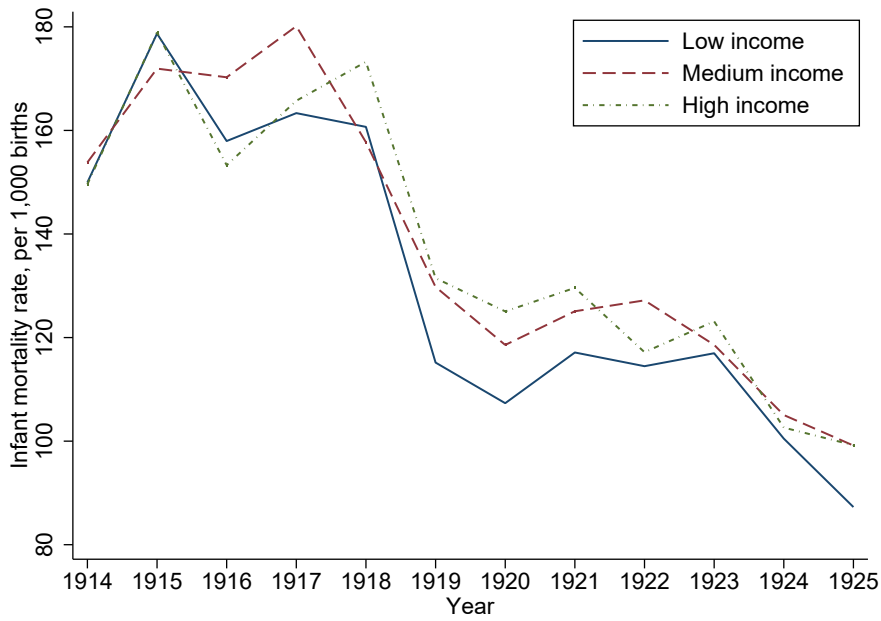


**Figure A-8:** Infant mortality rate 1914–1925 by income tercile

*Notes:* The figure shows the annual average infant mortality rate per 1,000 births in parishes for the years 1914 to 1925 by terciles of income 1907. *Sources:* Königliches Statistisches Landesamt (1910), Statistisches Landesamt Baden-Württemberg (2008), Staatsarchiv Ludwigsburg E 258 VII Bü 120 and 122. Author's design.

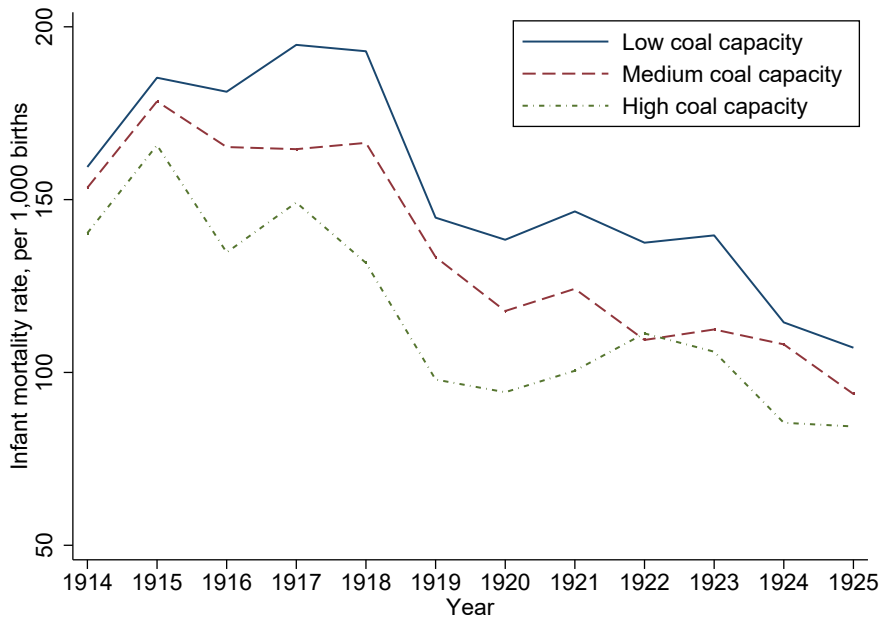


**Figure A-9:** Infant mortality rate 1914–1925 by coal capacity tercile

*Notes:* The figure shows the annual average infant mortality rate per 1,000 births in parishes for the years 1914 to 1925 by terciles of installed coal-fired power plant capacity within 50 kilometers. *Sources:* Ott et al. (1981), Statistisches Landesamt Baden-Württemberg (2008), Staatsarchiv Ludwigsburg E 258 VII Bü 120 and 122. Author's design.

## A.6 Tables

**Table A-4:** Baseline results – DiD Estimates – Full

... × 1918	Mortality rate 1914–1925					
	(1)	(2)	(3)	(4)	(5)	(6)
Income medium	-1.710*** (0.482)	-1.378*** (0.466)			-1.638*** (0.494)	-1.379*** (0.473)
Income high	-1.277*** (0.463)	-0.993* (0.526)			-1.147** (0.494)	-0.969* (0.526)
Coal medium			-0.045 (0.533)	-0.101 (0.597)	-0.320 (0.528)	-0.202 (0.590)
Coal high			1.062** (0.425)	1.056* (0.564)	0.715 (0.445)	0.958* (0.569)
Pop. 1910, log		0.127 (0.254)		0.093 (0.253)		0.154 (0.247)
Pop. density 1910		0.432 (0.384)		0.473 (0.384)		0.271 (0.388)
Ind. empl. 1905, share		-0.009 (0.028)		-0.033 (0.026)		-0.013 (0.027)
Average firm size 1895		0.005 (0.108)		-0.006 (0.103)		-0.003 (0.104)
Hydro capacity, MW		0.024 (0.016)		0.020 (0.016)		0.017 (0.016)
Birth non local 1900, share		3.745** (1.535)		3.548** (1.533)		4.224*** (1.508)
Railway station 1910, dummy		-0.981*** (0.347)		-1.025*** (0.350)		-0.952*** (0.348)
Road access 1848, dummy		-0.228 (0.323)		-0.259 (0.332)		-0.239 (0.321)
River access, dummy		-0.633 (0.489)		-0.803* (0.466)		-0.564 (0.497)
Dist. WWI base, km		-0.017 (0.057)		0.004 (0.056)		-0.004 (0.057)
Observations	21,156	21,156	21,156	21,156	21,156	21,156
FE	Yes	Yes	Yes	Yes	Yes	Yes
Year FE	Yes	Yes	Yes	Yes	Yes	Yes
Year × District FE	No	Yes	No	Yes	No	Yes

*Notes:* The table shows panel regression estimates of the effect of taxable income 1907 and installed coal-fired power plant capacity within 50 kilometers on the differential change in mortality rates. Regressions (1) and (2) show the change in medium and high-income parishes between 1917 and 1918 relative to the change in low-income parishes. Regressions (3) and (4) show the change in medium and high coal capacity parishes between 1917 and 1918 relative to the change in low coal capacity parishes. Regressions (5) and (6) include income and coal capacity measures. All regressions include a full set of year, parish fixed effects, and the average mortality rate 1910–1913 interacted with year fixed effects. Columns (2), (4), and (6) include the full set of pre-treatment control variables  $X_i$  each interacted with an indicator variable for the year 1918 and year times district fixed effects. Standard errors clustered at the county level are in parentheses. \*\*\*, \*\*, and \* denote statistical significance at the 1, 5, and 10 percent level, respectively.

**Table A-5: Robustness – Baseline year 1914**

	Mortality rate 1914–1925					
	(1)	(2)	(3)	(4)	(5)	(6)
Income medium $\times$ 1918	-1.980*** (0.476)	-1.705*** (0.524)			-1.862*** (0.487)	-1.683*** (0.530)
Income high $\times$ 1918	-1.823*** (0.557)	-1.669** (0.659)			-1.605*** (0.555)	-1.603** (0.657)
Coal medium $\times$ 1918			0.218 (0.662)	0.239 (0.630)	-0.165 (0.640)	0.057 (0.622)
Coal high $\times$ 1918			1.483** (0.564)	1.487** (0.628)	1.003* (0.555)	1.298** (0.623)
Observations	21,156	21,156	21,156	21,156	21,156	21,156
FE	Yes	Yes	Yes	Yes	Yes	Yes
Year FE	Yes	Yes	Yes	Yes	Yes	Yes
Controls	No	Yes	No	Yes	No	Yes
Year $\times$ District FE	No	Yes	No	Yes	No	Yes

*Notes:* The table shows panel regression estimates of the effect of taxable income 1907 and installed coal-fired power plant capacity within 50 kilometers on the differential change in mortality rates. Regressions (1) and (2) show the change in medium and high-income parishes between 1914 and 1918 relative to the change in low-income parishes. Regressions (3) and (4) show the change in medium and high coal capacity parishes between 1914 and 1918 relative to the change in low coal capacity parishes. Regressions (5) and (6) include income and coal capacity measures. All regressions include a full set of year fixed effects, parish fixed effects, and the average mortality rate 1910–1913 interacted with year fixed effects. Columns (2), (4), and (6) include the full set of pre-treatment control variables  $X_i$  each interacted with an indicator variable for the year 1918 and year times district fixed effects. Standard errors clustered at the county level are in parentheses. \*\*\*, \*\*, and \* denote statistical significance at the 1, 5, and 10 percent level, respectively.

**Table A-6: Robustness checks – Include infant mortality**

	All-age mortality rate 1914–1925					
	(1)	(2)	(3)	(4)	(5)	(6)
Income medium $\times$ 1918	-1.739*** (0.576)	-1.555*** (0.555)			-1.702*** (0.578)	-1.545*** (0.561)
Income high $\times$ 1918	-1.053** (0.518)	-1.141** (0.560)			-0.987* (0.530)	-1.095* (0.565)
Coal medium $\times$ 1918			-0.125 (0.548)	0.062 (0.594)	-0.363 (0.541)	-0.048 (0.590)
Coal high $\times$ 1918			0.769* (0.460)	1.013* (0.601)	0.467 (0.470)	0.905 (0.603)
Observations	21,156	21,156	21,156	21,156	21,156	21,156
FE	Yes	Yes	Yes	Yes	Yes	Yes
Year FE	Yes	Yes	Yes	Yes	Yes	Yes
Controls	No	Yes	No	Yes	No	Yes
Year $\times$ District FE	No	Yes	No	Yes	No	Yes

*Notes:* The table shows panel regression estimates of the effect of taxable income 1907 and installed coal-fired power plant capacity within 50 kilometers on the differential change in all-age mortality rates, i.e., including infant mortality. Regressions (1) and (2) show the change in medium and high-income parishes between 1917 and 1918 relative to the change in low-income parishes. Regressions (3) and (4) show the change in medium and high coal capacity parishes between 1917 and 1918 relative to the change in low coal capacity parishes. Regressions (5) and (6) include income and coal capacity measures. All regressions include a full set of year fixed effects, parish fixed effects, and the average mortality rate 1910–1913 interacted with year fixed effects. Columns (2), (4), and (6) include the full set of pre-treatment control variables  $X_i$  each interacted with an indicator variable for the year 1918 and year times district fixed effects. Standard errors clustered at the county level are in parentheses. \*\*\*, \*\*, and \* denote statistical significance at the 1, 5, and 10 percent level, respectively.

**Table A-7: Robustness checks – Control for WWI**

	Mortality rate					
	(1)	(2)	(3)	(4)	(5)	(6)
<b>Panel A: WWI years only</b>						
Income medium $\times$ 1918	-1.710*** (0.482)	-1.368*** (0.472)			-1.638*** (0.493)	-1.370*** (0.478)
Income high $\times$ 1918	-1.277*** (0.463)	-1.119** (0.557)			-1.147** (0.494)	-1.098* (0.557)
Coal medium $\times$ 1918			-0.045 (0.533)	-0.034 (0.599)	-0.320 (0.528)	-0.148 (0.594)
Coal high $\times$ 1918			1.062** (0.425)	1.120* (0.566)	0.715 (0.445)	1.004* (0.573)
Observations	8,815	8,815	8,815	8,815	8,815	8,815
<b>Panel B: Control for deaths of military personnel</b>						
Income medium $\times$ 1918	-1.712*** (0.480)	-1.382*** (0.464)			-1.638*** (0.491)	-1.384*** (0.470)
Income high $\times$ 1918	-1.272*** (0.460)	-0.991* (0.523)			-1.139** (0.490)	-0.967* (0.522)
Coal medium $\times$ 1918			-0.058 (0.529)	-0.119 (0.592)	-0.331 (0.524)	-0.219 (0.584)
Coal high $\times$ 1918			1.074** (0.423)	1.059* (0.561)	0.728 (0.443)	0.960* (0.566)
Observations	21,156	21,156	21,156	21,156	21,156	21,156
FE	Yes	Yes	Yes	Yes	Yes	Yes
Year FE	Yes	Yes	Yes	Yes	Yes	Yes
Controls	No	Yes	No	Yes	No	Yes
Year $\times$ District FE	No	Yes	No	Yes	No	Yes

*Notes:* The table shows panel regression estimates of the effect of taxable income 1907 and installed coal-fired power plant capacity within 50 kilometers on the differential change in mortality rates. In Panel A the sample is reduced to include WWI years 1914–1918 only. Panel B includes the annual number of deaths of military personnel at the parish level as control variable. Regressions (1) and (2) show the change in medium and high-income parishes between 1917 and 1918 relative to the change in low-income parishes. Regressions (3) and (4) show the change in medium and high coal capacity parishes between 1917 and 1918 relative to the change in low coal capacity parishes. Regressions (5) and (6) include income and coal capacity measures. All regressions include a full set of year fixed effects, parish fixed effects, and the average mortality rate 1910–1913 interacted with year fixed effects. Columns (2), (4), and (6) include the full set of pre-treatment control variables  $X_i$  each interacted with an indicator variable for the year 1918 and year times district fixed effects. Standard errors clustered at the county level are in parentheses. \*\*\*, \*\*, and \* denote statistical significance at the 1, 5, and 10 percent level, respectively.

**Table A-8:** Robustness checks – Include Bavarian coal-fired power plants

	Mortality rate 1914–1925			
	(1)	(2)	(3)	(4)
Income medium $\times$ 1918			-1.645***	-1.388***
			(0.493)	(0.472)
Income high $\times$ 1918			-1.160**	-0.980*
			(0.495)	(0.527)
Coal medium $\times$ 1918	-0.101	-0.153	-0.378	-0.260
	(0.527)	(0.589)	(0.523)	(0.582)
Coal high $\times$ 1918	1.034**	1.034*	0.684	0.928
	(0.421)	(0.561)	(0.442)	(0.567)
Observations	21,156	21,156	21,156	21,156
FE	Yes	Yes	Yes	Yes
Year FE	Yes	Yes	Yes	Yes
Controls	No	Yes	No	Yes
Year $\times$ District FE	No	Yes	No	Yes

*Notes:* The table shows panel regression estimates of the effect of taxable income 1907 and installed coal-fired power plant capacity within 50 kilometers on the differential change in mortality rates. The power plant data include Bavarian coal-fired power plants listed in Dettmar (1913). Regressions (1) and (2) show the change in medium and high coal capacity parishes between 1917 and 1918 relative to the change in low coal capacity parishes. Regressions (3) and (4) include income and coal capacity measures. All regressions include a full set of year fixed effects, parish fixed effects, and the average mortality rate 1910–1913 interacted with year fixed effects. Columns (2) and (4) include the full set of pre-treatment control variables  $X_i$  each interacted with an indicator variable for the year 1918 and year times district fixed effects. Standard errors clustered at the county level are in parentheses. \*\*\*, \*\*, and \* denote statistical significance at the 1, 5, and 10 percent level, respectively.

**Table A-9:** Robustness checks – Controls interacted with Year FE

	Mortality rate 1914–1925		
	(1)	(2)	(3)
Income medium $\times$ 1918	-1.292*** (0.480)		-1.296*** (0.483)
Income high $\times$ 1918	-0.761 (0.574)		-0.739 (0.572)
Coal medium $\times$ 1918		-0.115 (0.601)	-0.214 (0.598)
Coal high $\times$ 1918		1.060* (0.586)	0.970 (0.591)
Observations	21,156	21,156	21,156
FE	Yes	Yes	Yes
Year FE	Yes	Yes	Yes
Controls	Yes	Yes	Yes
Year $\times$ District FE	Yes	Yes	Yes

*Notes:* The table shows panel regression estimates of the effect of taxable income 1907 and installed coal-fired power plant capacity within 50 kilometers on the differential change in mortality rates. Regression (1) shows the change in medium and high-income parishes between 1917 and 1918 relative to the change in low-income parishes. Regression (2) shows the change in medium and high coal capacity parishes between 1917 and 1918 relative to the change in low coal capacity parishes. Regression (3) includes income and coal capacity measures. All regressions include a full set of year fixed effects, parish fixed effects, the average mortality rate 1910–1913 interacted with year fixed effects, the full set of pre-treatment control variables  $X_i$  each interacted with year fixed effects, and year times district fixed effects. Standard errors clustered at the county level are in parentheses. \*\*\*, \*\*, and \* denote statistical significance at the 1, 5, and 10 percent level, respectively.

**Table A-10:** Robustness checks – Quintiles

	Mortality rate 1914–1925					
	(1)	(2)	(3)	(4)	(5)	(6)
Income medium-low $\times$ 1918	-1.077*	-0.888			-0.967	-0.836
	(0.638)	(0.617)			(0.650)	(0.632)
Income medium $\times$ 1918	-2.316***	-1.968***			-2.164***	-1.933**
	(0.730)	(0.738)			(0.775)	(0.774)
Income medium-high $\times$ 1918	-1.234*	-0.816			-0.936	-0.712
	(0.629)	(0.699)			(0.669)	(0.715)
Income high $\times$ 1918	-1.906**	-1.794**			-1.631**	-1.728**
	(0.717)	(0.831)			(0.780)	(0.861)
Coal medium-low $\times$ 1918			0.400	0.281	0.328	0.421
			(0.689)	(0.704)	(0.677)	(0.697)
Coal medium $\times$ 1918			0.238	0.045	-0.048	0.016
			(0.695)	(0.814)	(0.677)	(0.789)
Coal medium-high $\times$ 1918			1.591***	1.734**	1.325**	1.737**
			(0.572)	(0.688)	(0.575)	(0.679)
Coal high $\times$ 1918			1.289***	1.280	0.894	1.205
			(0.483)	(0.794)	(0.538)	(0.826)
Observations	21,156	21,156	21,156	21,156	21,156	21,156
FE	Yes	Yes	Yes	Yes	Yes	Yes
Year FE	Yes	Yes	Yes	Yes	Yes	Yes
Controls	No	Yes	No	Yes	No	Yes
Year $\times$ District FE	No	Yes	No	Yes	No	Yes

*Notes:* The table shows panel regression estimates of the effect of taxable income 1907 and installed coal-fired power plant capacity within 50 kilometers on the differential change in mortality rates. Regressions (1) and (2) show the change in medium-low, medium, medium-high, and high-income parishes between 1917 and 1918 relative to the change in low-income parishes. Regressions (3) and (4) show the change in medium-low, medium, medium-high, and high coal capacity parishes between 1917 and 1918 relative to the change in low coal capacity parishes. Regressions (5) and (6) include income and coal capacity measures. All regressions include a full set of year fixed effects, parish fixed effects, and the average mortality rate 1910–1913 interacted with year fixed effects. Columns (2), (4), and (6) include the full set of pre-treatment control variables  $X_i$  each interacted with an indicator variable for the year 1918 and year times district fixed effects. Standard errors clustered at the county level are in parentheses. \*\*\*, \*\*, and \* denote statistical significance at the 1, 5, and 10 percent level, respectively.

**Table A-11:** Robustness checks – Exclude large and small parishes by population 1910

	Mortality rate 1914–1925					
	(1)	(2)	(3)	(4)	(5)	(6)
<b>Panel A:</b> Exclude largest and smallest one percent of parishes						
Income medium $\times$ 1918	-1.748*** (0.475)	-1.469*** (0.453)			-1.675*** (0.485)	-1.459*** (0.461)
Income high $\times$ 1918	-1.360*** (0.437)	-1.162** (0.512)			-1.227** (0.469)	-1.126** (0.511)
Coal medium $\times$ 1918			-0.085 (0.550)	-0.021 (0.615)	-0.385 (0.545)	-0.137 (0.605)
Coal high $\times$ 1918			1.108** (0.435)	1.190** (0.590)	0.727 (0.456)	1.065* (0.592)
Observations	20,748	20,748	20,748	20,748	20,748	20,748
<b>Panel B:</b> Exclude largest and smallest 5 percent of parishes						
Income medium $\times$ 1918	-1.591*** (0.459)	-1.266*** (0.447)			-1.496*** (0.472)	-1.222*** (0.455)
Income high $\times$ 1918	-1.096** (0.478)	-0.846 (0.550)			-0.905* (0.528)	-0.765 (0.555)
Coal medium $\times$ 1918			0.043 (0.538)	0.296 (0.613)	-0.187 (0.551)	0.203 (0.605)
Coal high $\times$ 1918			1.074** (0.454)	1.385** (0.638)	0.772 (0.494)	1.281* (0.644)
Observations	19,044	19,044	19,044	19,044	19,044	19,044
FE	Yes	Yes	Yes	Yes	Yes	Yes
Year FE	Yes	Yes	Yes	Yes	Yes	Yes
Controls	No	Yes	No	Yes	No	Yes
Year $\times$ District FE	No	Yes	No	Yes	No	Yes

*Notes:* The table shows panel regression estimates of the effect of taxable income 1907 and installed coal-fired power plant capacity within 50 kilometers on the differential change in mortality rates. Panel A (Panel B) shows results based on a sample excluding the smallest and largest one (five) percent of parishes based on population size 1910. Regressions (1) and (2) show the change in medium and high-income parishes between 1917 and 1918 relative to the change in low-income parishes. Regressions (3) and (4) show the change in medium and high coal capacity parishes between 1917 and 1918 relative to the change in low coal capacity parishes. Regressions (5) and (6) include income and coal capacity measures. All regressions include a full set of year fixed effects, parish fixed effects, and the average mortality rate 1910–1913 interacted with year fixed effects. Columns (2), (4), and (6) include the full set of pre-treatment control variables  $X_i$  each interacted with an indicator variable for the year 1918 and year times district fixed effects. Standard errors clustered at the county level are in parentheses. \*\*\*, \*\*, and \* denote statistical significance at the 1, 5, and 10 percent level, respectively.

**Table A-12:** Robustness checks – Conley S.E.

	Mortality rate 1914–1925					
	(1)	(2)	(3)	(4)	(5)	(6)
Income medium × 1918	-1.770*** (0.484) [0.436] {0.384}	-1.449*** (0.498) [0.436] {0.381}			-1.695*** (0.485) [0.439] {0.388}	-1.447*** (0.499) [0.438] {0.389}
Income high × 1918	-1.211** (0.475) [0.480] {0.502}	-0.936* (0.559) [0.543] {0.524}			-1.076** (0.481) [0.490] {0.455}	-0.911 (0.558) [0.543] {0.516}
Coal medium × 1918			-0.049 (0.491) [0.494] {0.527}	-0.101 (0.551) [0.524] {0.490}	-0.306 (0.493) [0.476] {0.447}	-0.191 (0.550) [0.518] {0.466}
Coal high × 1918			1.058** (0.452) [0.452] {0.499}	1.088* (0.606) [0.569] {0.526}	0.733* (0.443) [0.439] {0.446}	0.999* (0.601) [0.567] {0.521}
Observations	21,097	21,097	21,097	21,097	21,097	21,097
FE	Yes	Yes	Yes	Yes	Yes	Yes
Year FE	Yes	Yes	Yes	Yes	Yes	Yes
Controls	No	Yes	No	Yes	No	Yes
Year × District FE	No	Yes	No	Yes	No	Yes

*Notes:* The table shows panel regression estimates of the effect of taxable income 1907 and installed coal-fired power plant capacity within 50 kilometers on the differential change in mortality rates. Regressions (1) and (2) show the change in medium and high-income parishes between 1917 and 1918 relative to the change in low-income parishes. Regressions (3) and (4) show the change in medium and high coal capacity parishes between 1917 and 1918 relative to the change in low coal capacity parishes. Regressions (5) and (6) include income and coal capacity measures. All regressions include a full set of year fixed effects, parish fixed effects, and the average mortality rate 1910–1913 interacted with year fixed effects. Columns (2), (4), and (6) include the full set of pre-treatment control variables  $X_i$  each interacted with an indicator variable for the year 1918 and year times district fixed effects. Conley standard errors with cut-off distances at 10 kilometers (in parentheses), 20 kilometers [in brackets], and 50 kilometers {in curly brackets} are below the point estimates. \*\*\*, \*\*, and \* denote the lowest statistical significance of all three specifications at the 1, 5, and 10 percent level, respectively.